Size Economy and First Hyperpolarizability. Synthesis and Nonlinear Optical Behavior of Ferrocene-based Donor-Acceptor Chromophores lacking π-Linker

Pawan Kumar,[a] Yovan de Coene,[b] Koen Clays,[b] Paramjit Kaur*,[a] and Kamaljit Singh*,[a]

[a]Department of Chemistry, UGC Centre of Advanced Study, Guru Nanak Dev University, Amritsar 143005, India. E-mail: kamaljit.chem@gndu.ac.in

[b]Department of Chemistry, University of Leuven, Celestijnenlaan 200D, B-3001 Leuven, Belgium. E-mail: Koen.Clays@fys.kuleuven.be

Table of Contents

Hyper Rayleigh scattering measurements and calculation of first hyperpolarizability.

(i) Calibration of solvent

It was done by internal reference method (IRM), wherein the dynamic hyperpolarizability of dichloromethane (DCM) was determined by measuring it against MeOH, a known reference (equation 1).[1]

$$<\beta_{HRS}>_{DCM} = \sqrt{\left(\frac{I_{2\omega,DCM}}{I_{2\omega,MeOH}}\right)\left(\frac{N_{DCM}}{N_{MeOH}}\right)\left(\frac{\left(n_{MeOH}^{2}+2\right)}{\left(n_{DCM}^{2}+2\right)}\right)^{6}} <\beta_{HRS}>_{MeOH} \quad (1)$$

(ii) Calibration of polarization sensitivity

For the accuracy of polarization sensitive measurements such as depolarization ratio, the polarization sensitivity (equation 2) of the grating and spectrometer for horizontally and vertically polarized light was taken into account. Thus, a spectrum of a white light source was recorded with a wire grid analyzer at both the horizontal and vertical position in front of the entrance slit of the spectrometer.

$$R_p = \frac{I_H}{I_V} \quad (2)$$

(iii) HRS measurements

Based on absorption and fluorescence emission of the compounds, concentrations (10^{-4}-10^{-6}M) were chosen considering the trade-off between resonance enhancement and self-absorption at the second-harmonic wavelength. A concentration series (5 concentrations + solvent) was made *in-situ* with the following dilution factors: 1,0.67,0.5,0.33 and 0.25 to give a broad range. 10 spectra were recorded for each concentration. These spectra were corrected for multiphoton fluorescence using a polynomial function. The 'fluorescence-free' spectrum was then fitted to a Gaussian function. Since 10 measurements were made at each concentration, the standard deviation on the Gaussian areas was taken as the error:

$$\sigma = \sqrt{\frac{\sum_{i=1}^{n}(y_i - \bar{y})^2}{n}} \qquad (3)$$

Subsequently, $I_{2\omega}$, normalized for the integration time were plotted as a function of the concentration. By performing a linear regression through the data points, we obtained a slope and intercept, where the intercept corresponded to the HRS intensity of the solvent. For the calculation of the error, we used a weighted fit where the weight of each data point was considered.

The hyperpolarizabilities were calculated using the internal reference method. For a two-component system, where solvent and solute both contribute to the HRS intensity,

$$I_{2\omega} = G\left(N_s < \beta_{HRS}^2 >_s + N_x < \beta_{HRS}^2 >_x\right) I_\omega^2 \qquad (4)$$

with N_s and N_x the number densities of the solvent and the solute respectively. The unknown hyperpolarizability of the solute ($< \beta_{HRS}^2 >_x$) was calculated by using the known value of the solvent ($< \beta_{HRS}^2 >_s$). By measuring $I_{2\omega}$ as a function of concentration, $<\beta_{HRS}>_x$ could be extracted by rewriting equation 4. By taking $GN_s < \beta_{HRS}^2 >_s$ as the intercept of the latter linear concentration dependence towards $I_{2\omega}$, and $G < \beta_{HRS}^2 >_x$ as the slope, yields the equation 5:

$$< \beta_{HRS} >_x = < \beta_{HRS} >_s \sqrt{\frac{slope}{intercept} N_s} \qquad (5)$$

To determine the error on $< \beta_{HRS} >_x$, standard error propagation rules were applied:

$$\sigma(< \beta_{HRS} >_x) = < \beta_{HRS} >_s \sqrt{N_s} \sqrt{\frac{1}{4\left(\frac{slope}{intercept}\right)}} \left(\left(\frac{1}{intercept}\right)^2 (\sigma_{slope})^2 + \left(-\frac{slope}{intercept^2} \right. \right. \qquad (6)$$

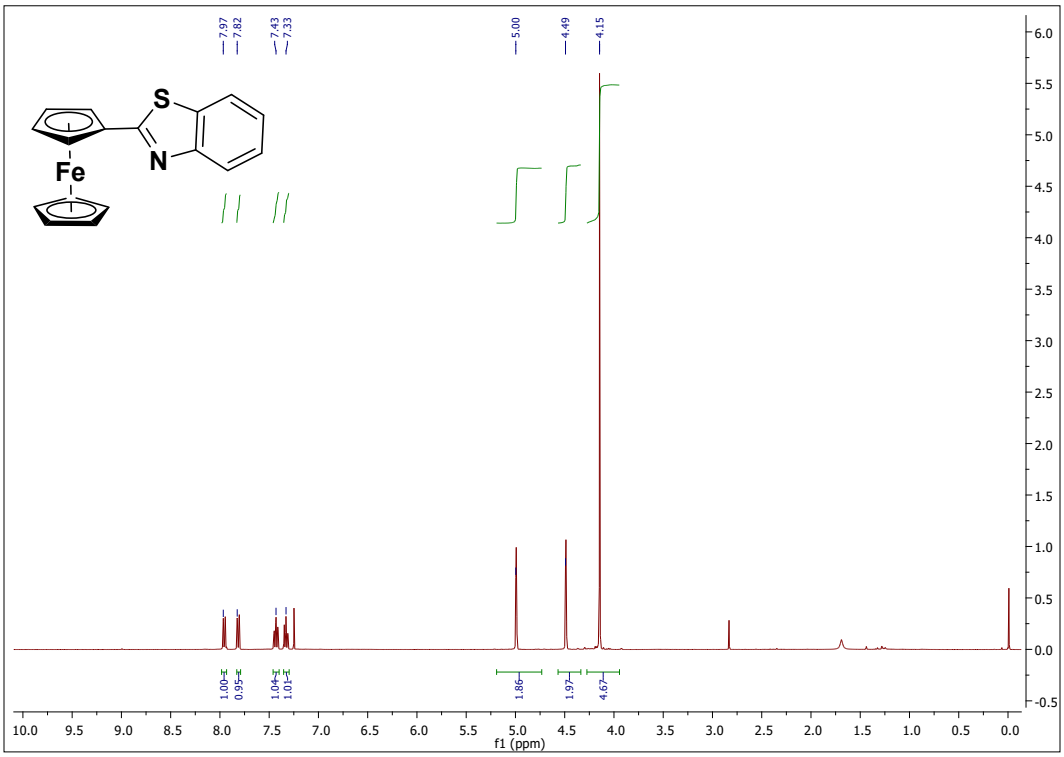

Figure S1. ^{1}H NMR spectrum (500 MHz, $CDCl_3$) of **2.**

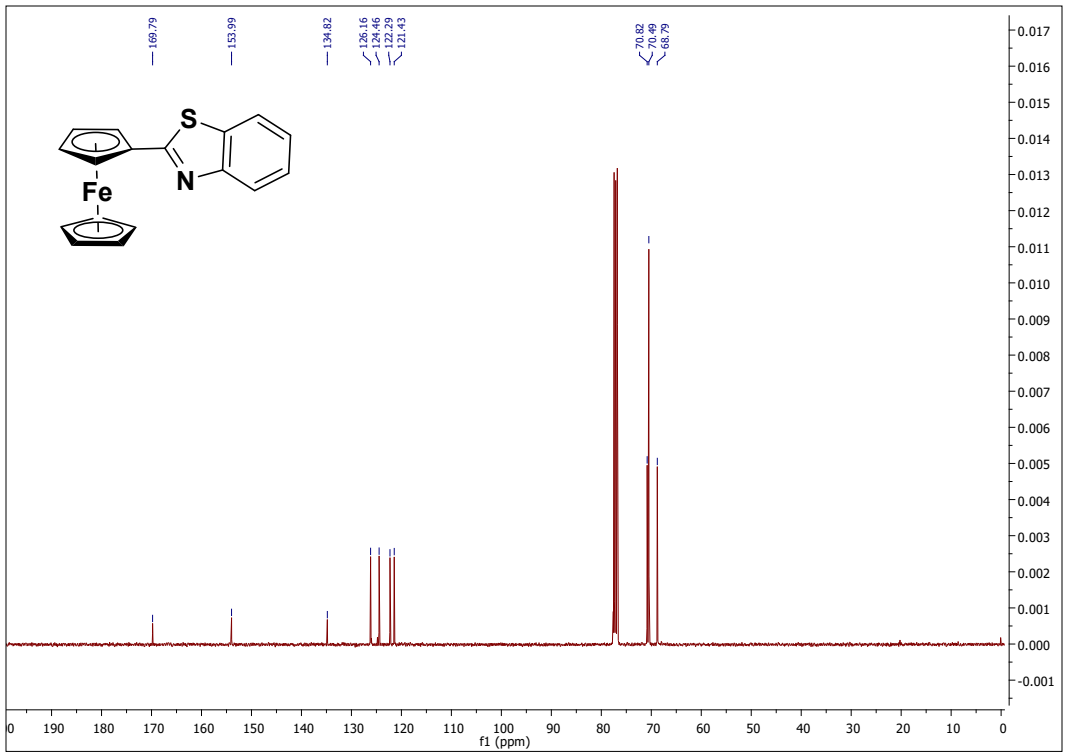

Figure S2. ^{13}C NMR spectrum (500 MHz, $CDCl_3$) of **2**.

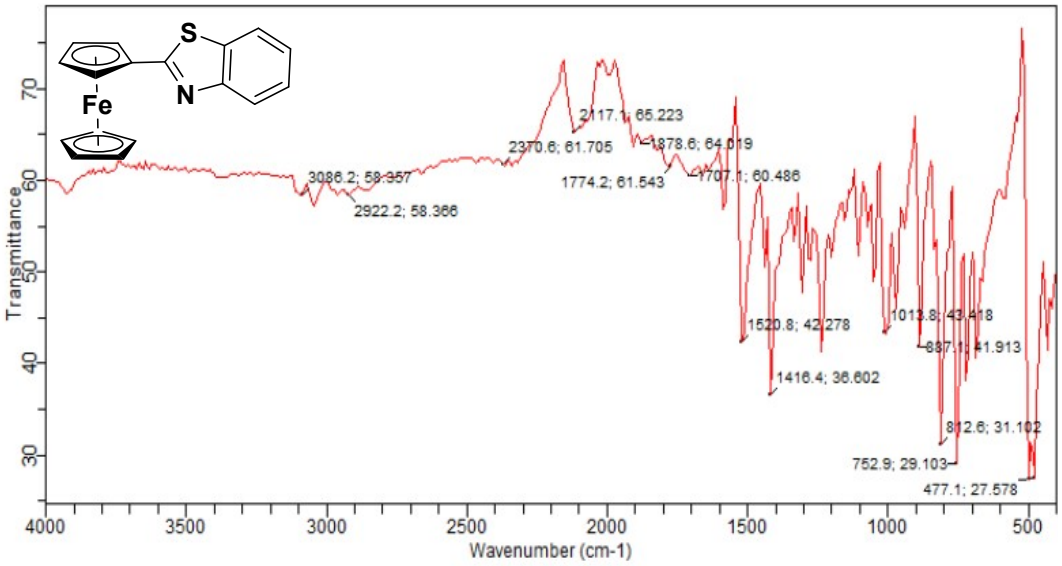

Figure S3. IR spectrum of **2**.

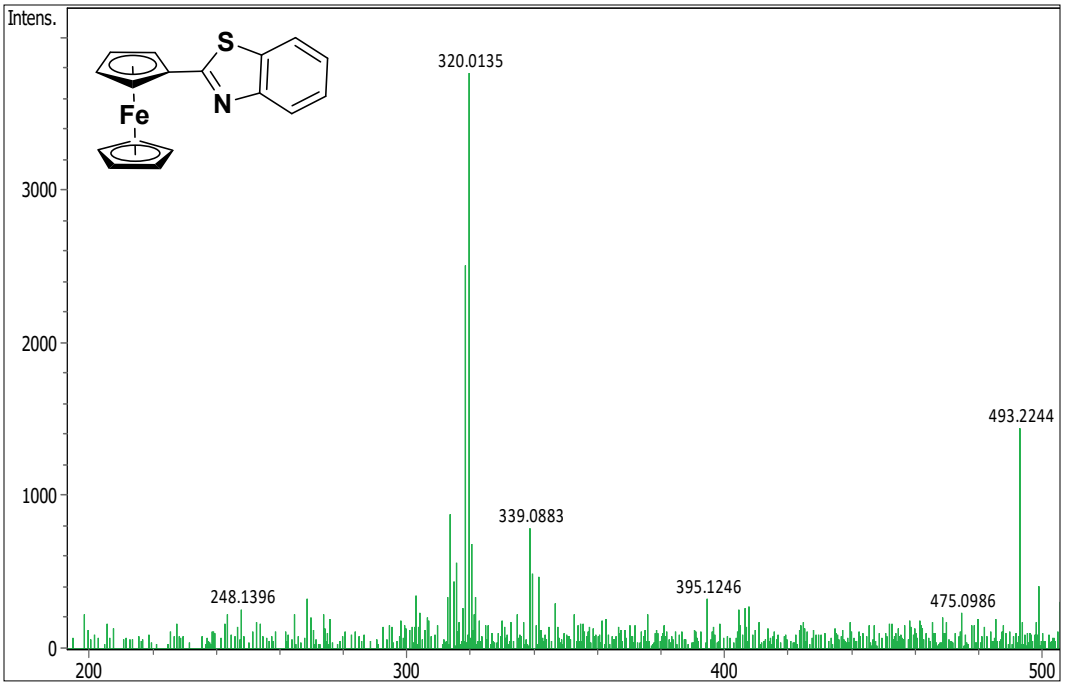

Figure S4. HRMS spectrum of **2**.

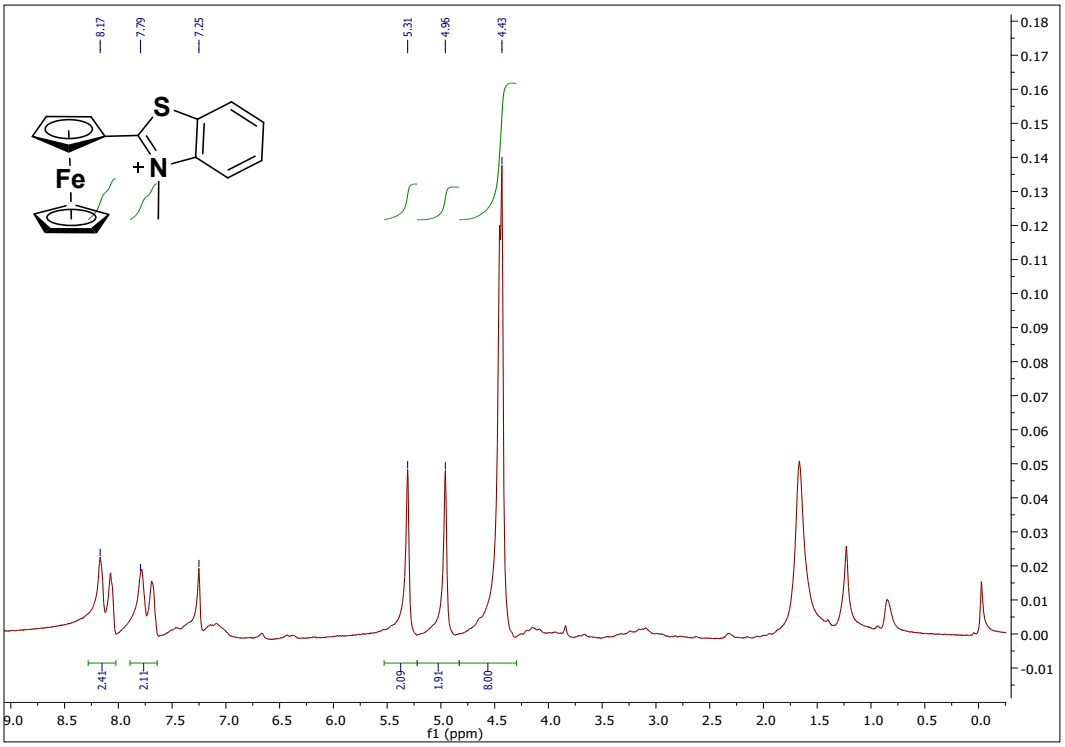

Figure S5. ^{1}H NMR spectrum (500 MHz, $CDCl_3$) of **3.**

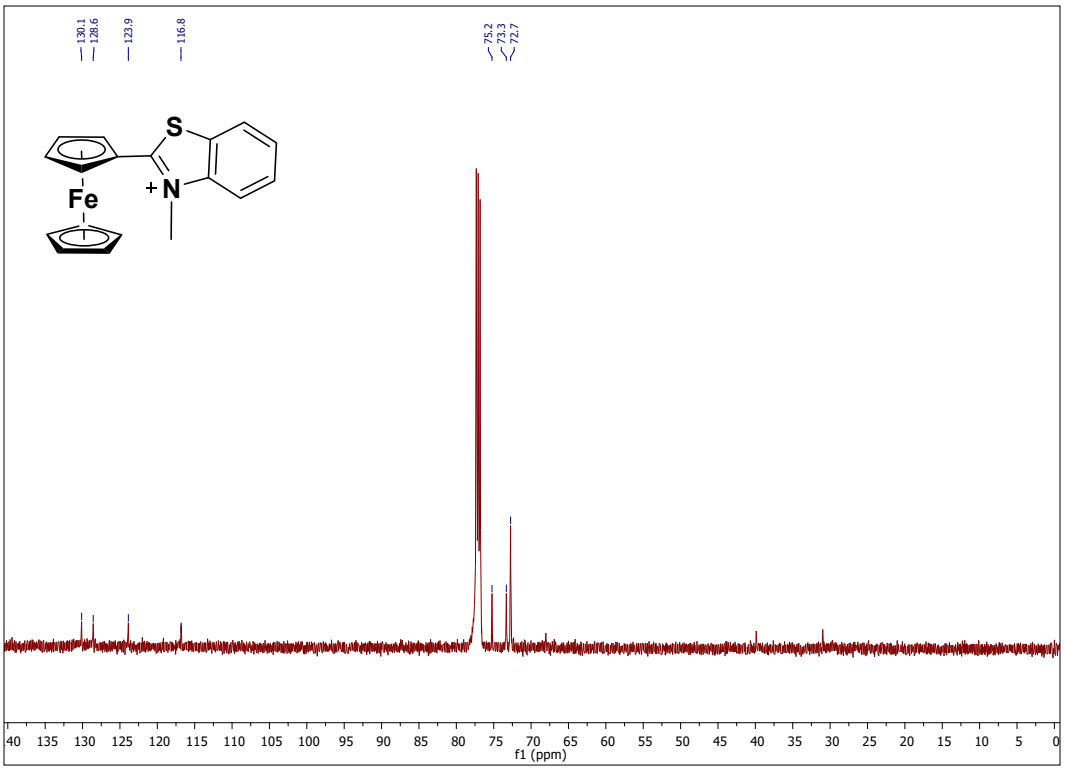

Figure S6. ^{13}C NMR spectrum (500 MHz, $CDCl_3$) of **3**.

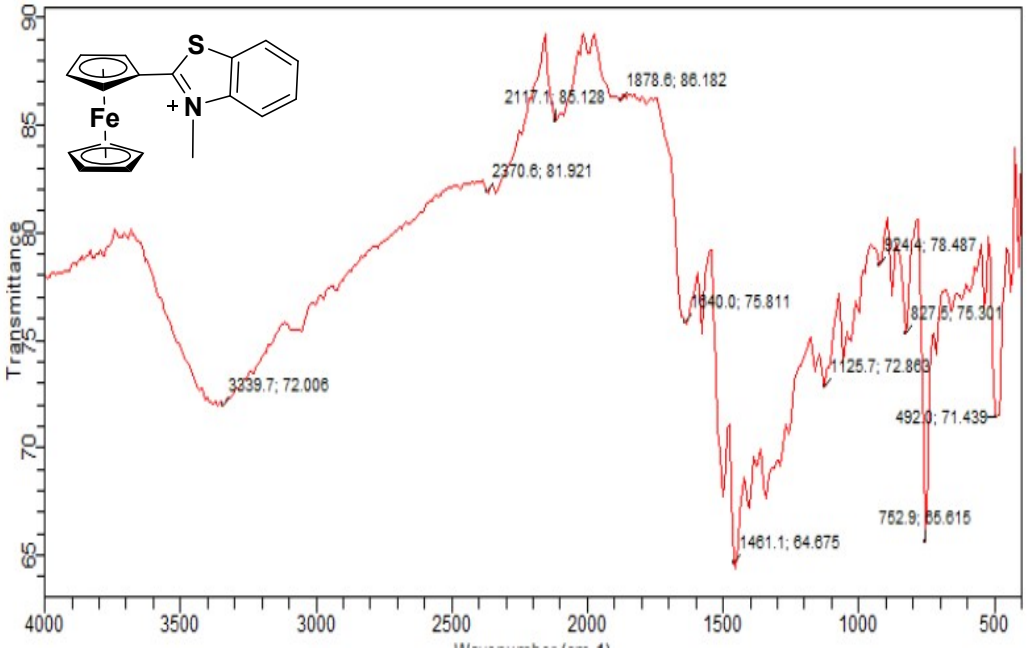

Figure S7. IR spectrum of **3**.

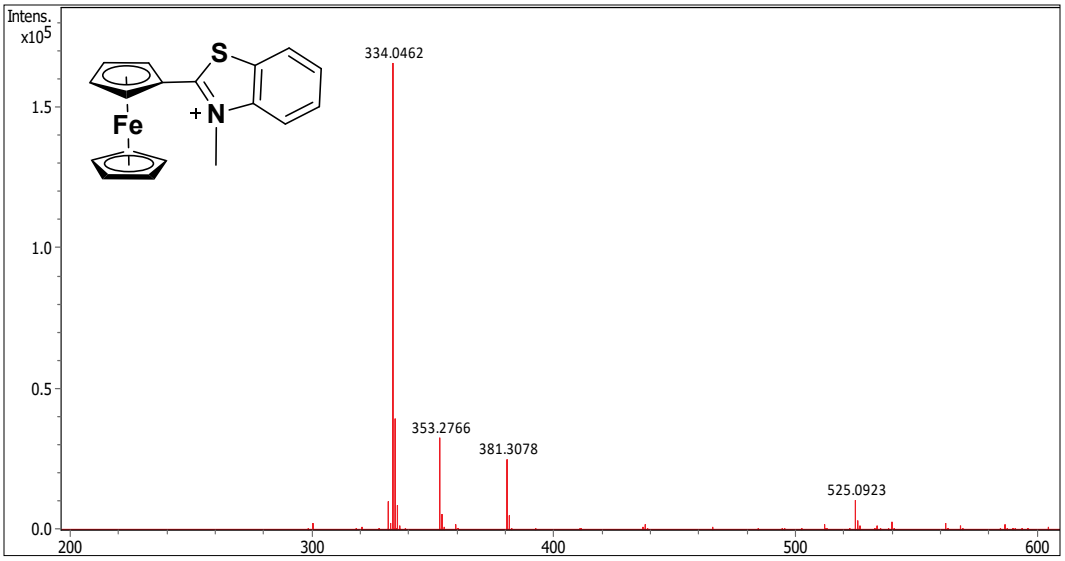

Figure S8. HRMS spectrum of **3**.

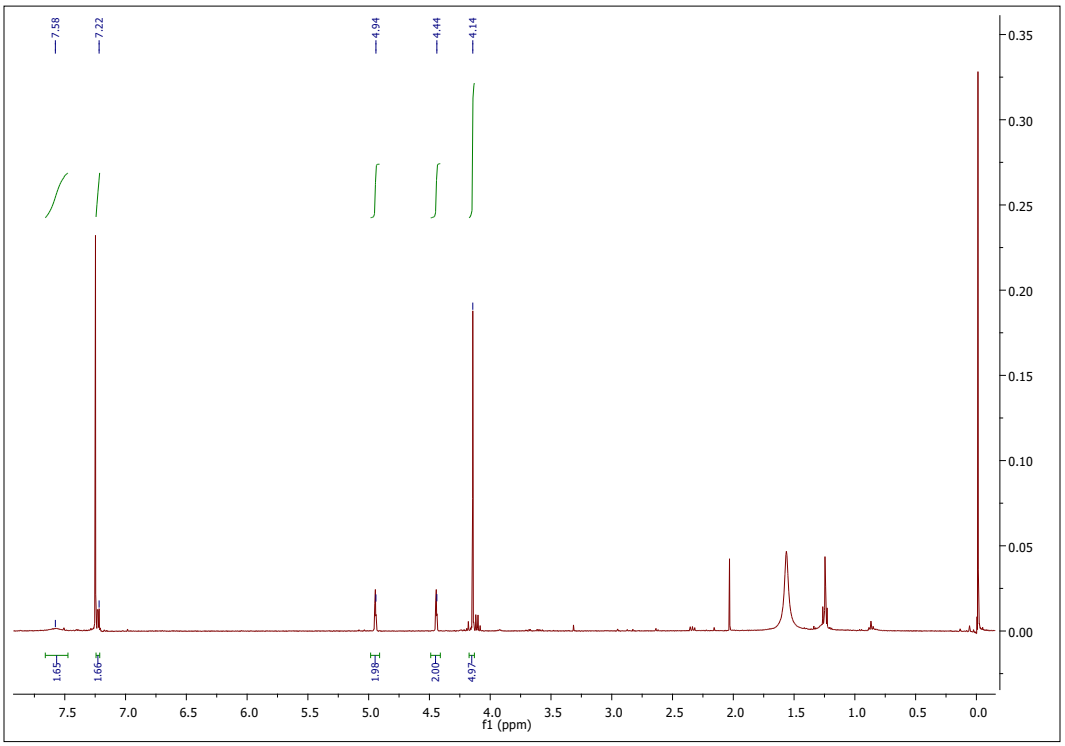

Figure S9. ^{1}H NMR spectrum (500 MHz, $CDCl_3$) of **4.**

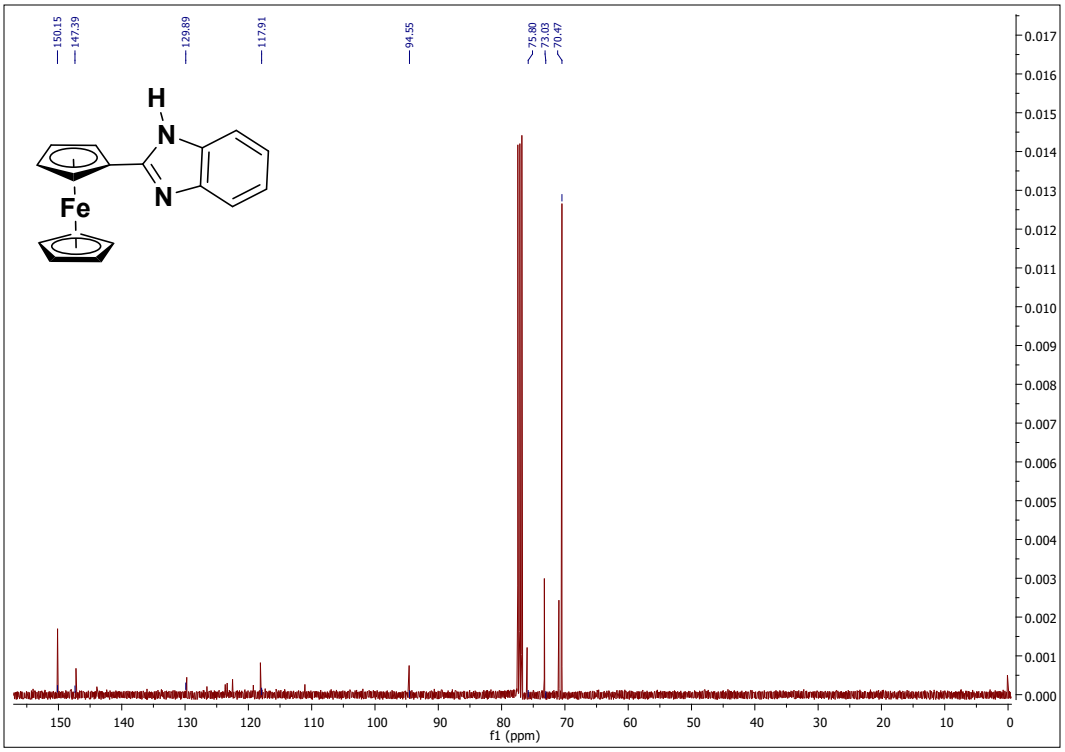

Figure S10. ^{13}C NMR spectrum (500 MHz, $CDCl_3$) of **4.**

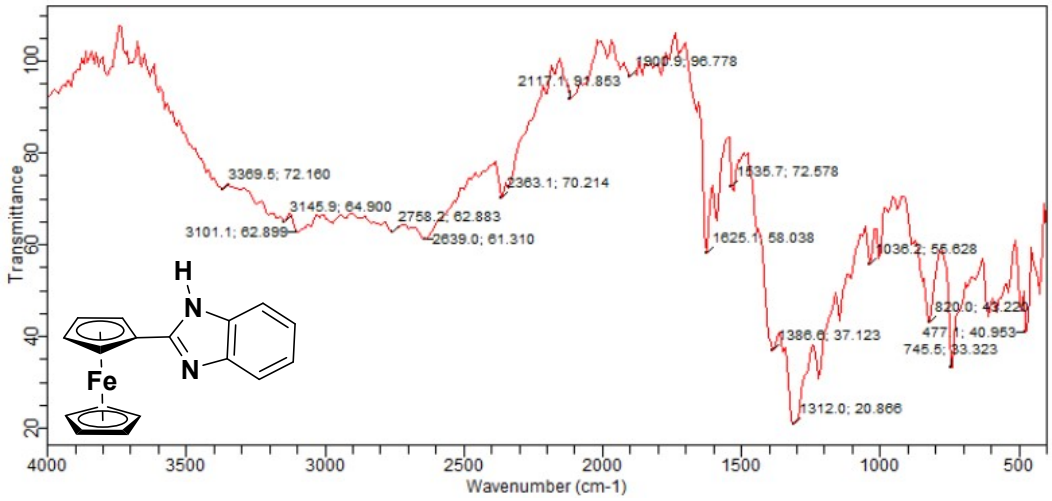

Figure S11. IR spectrum of **4.**

Figure S12. HRMS spectrum of **4.**

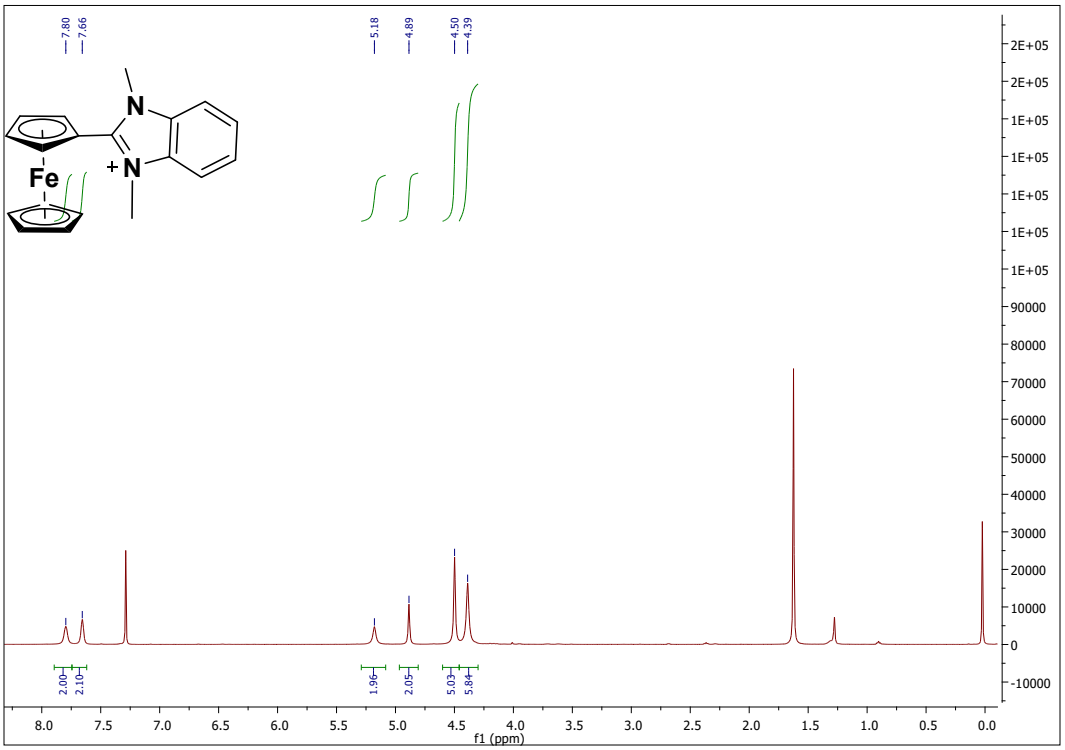

Figure S13. ^{1}H NMR spectrum (500 MHz, $CDCl_3$) of **5.**

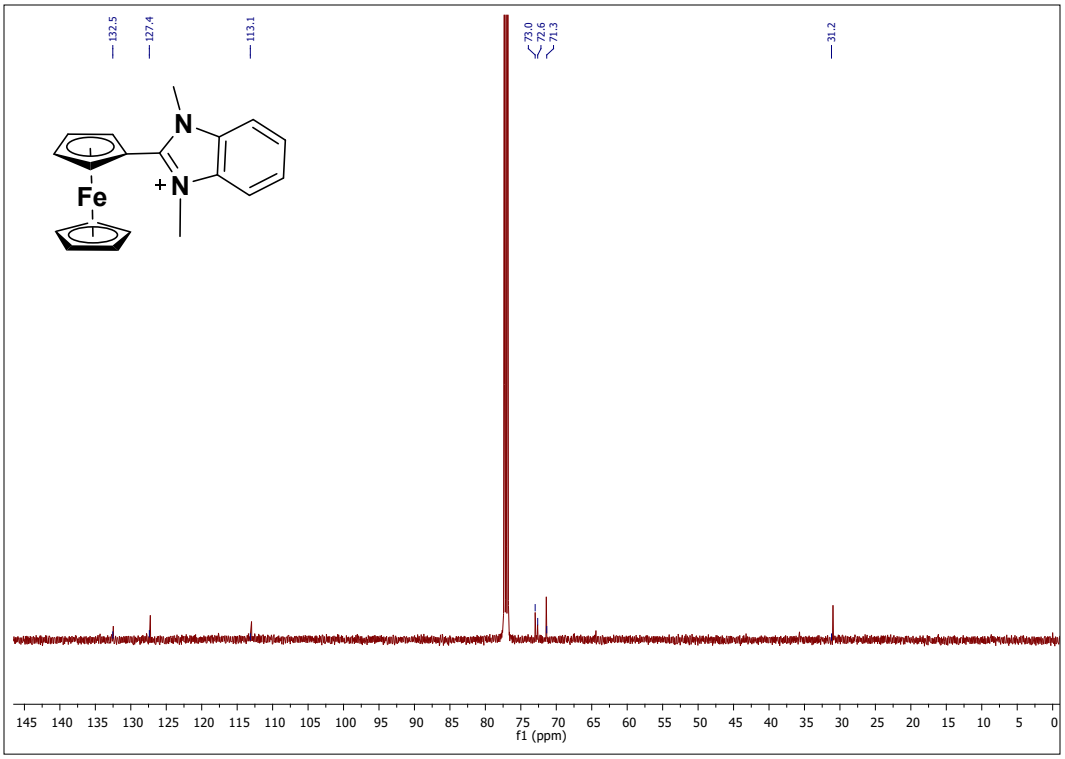

Figure S14. ^{13}C NMR spectrum (500 MHz, $CDCl_3$) of **5.**

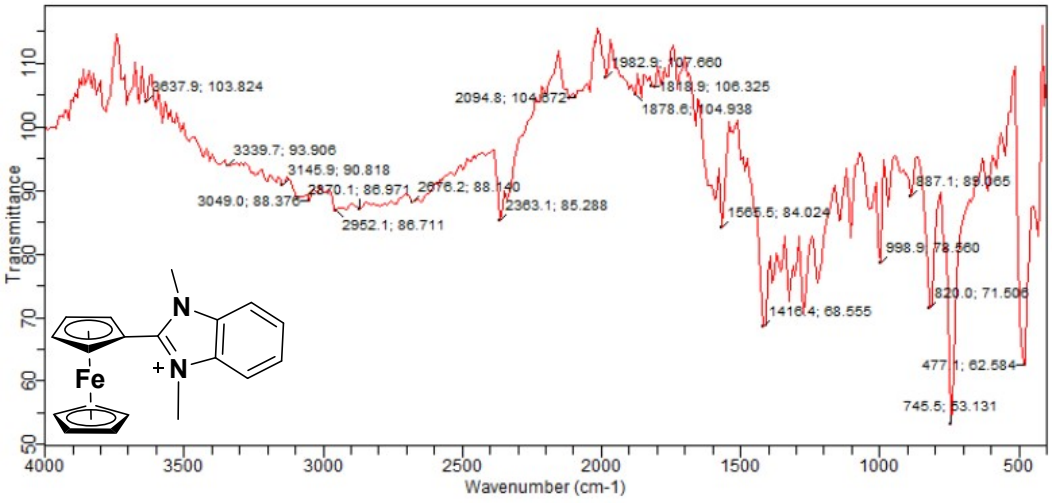

Figure S15. IR spectrum of **5.**

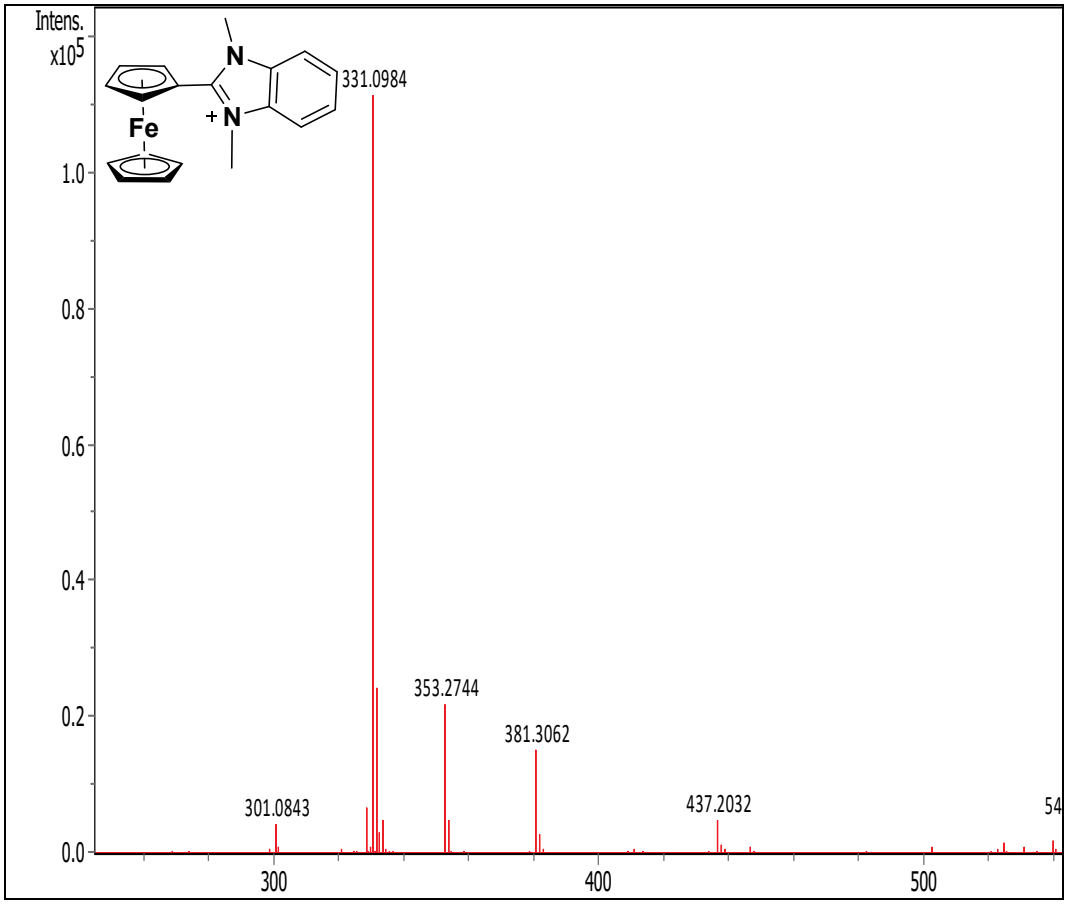

Figure S16. HRMS spectrum of **5.**

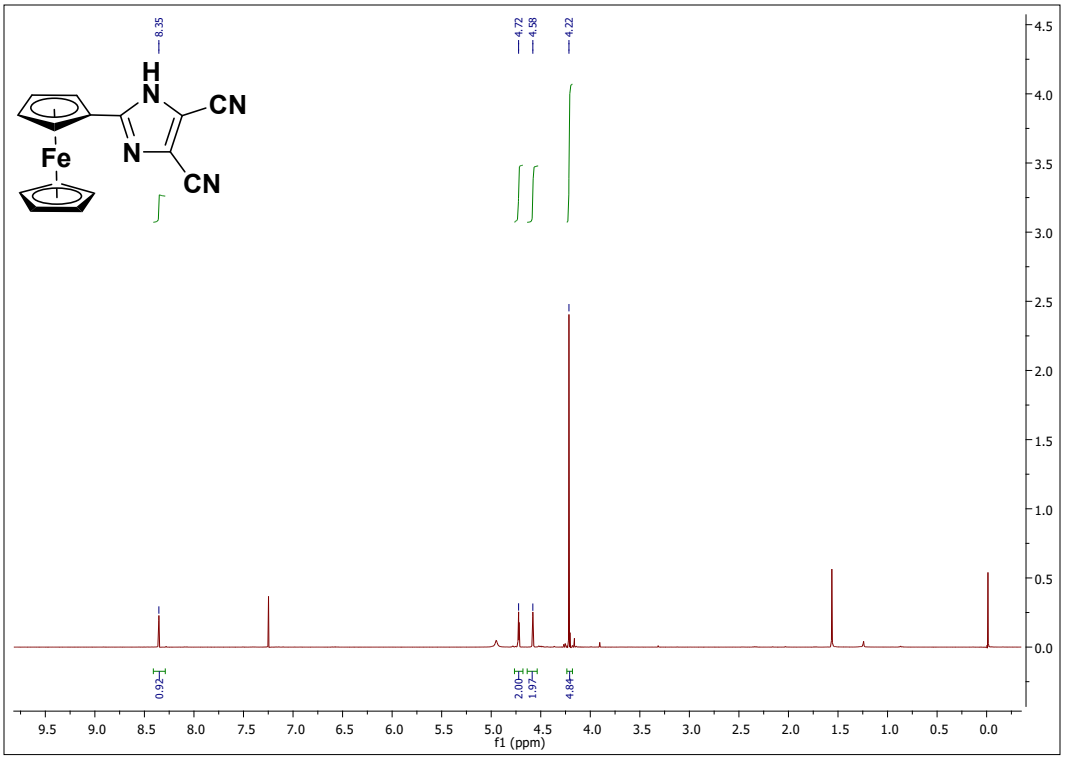

Figure S17. ^{1}H NMR spectrum (500 MHz, $CDCl_3$) of **6.**

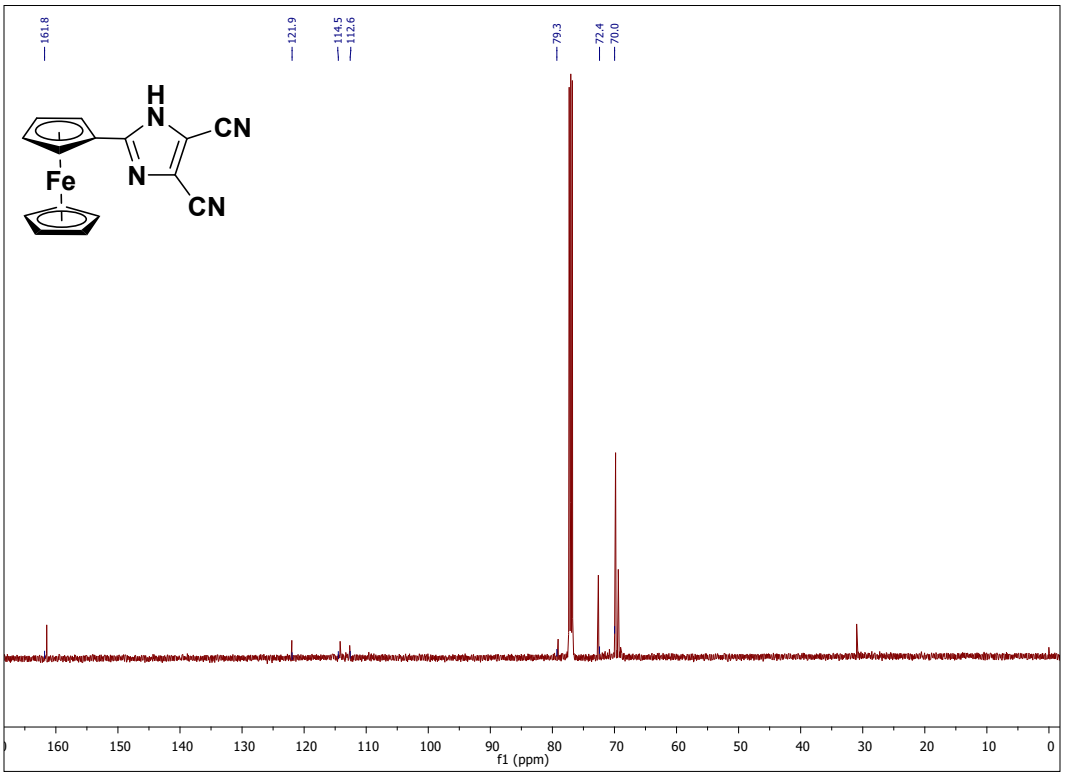

Figure S18. ^{13}C NMR spectrum (500 MHz, $CDCl_3$) of **6.**

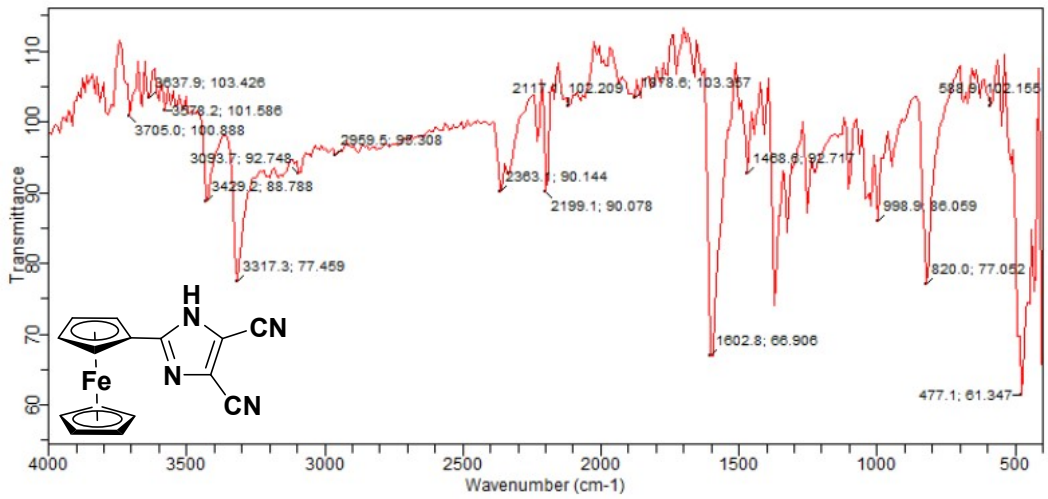

Figure S19. IR spectrum of **6.**

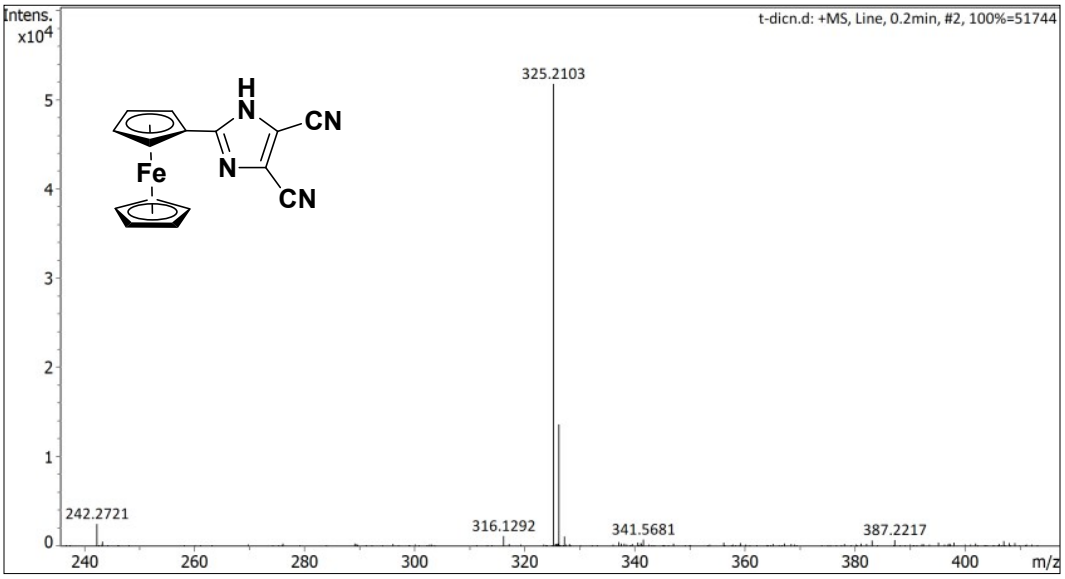

Figure S20. HRMS spectrum of **6.**

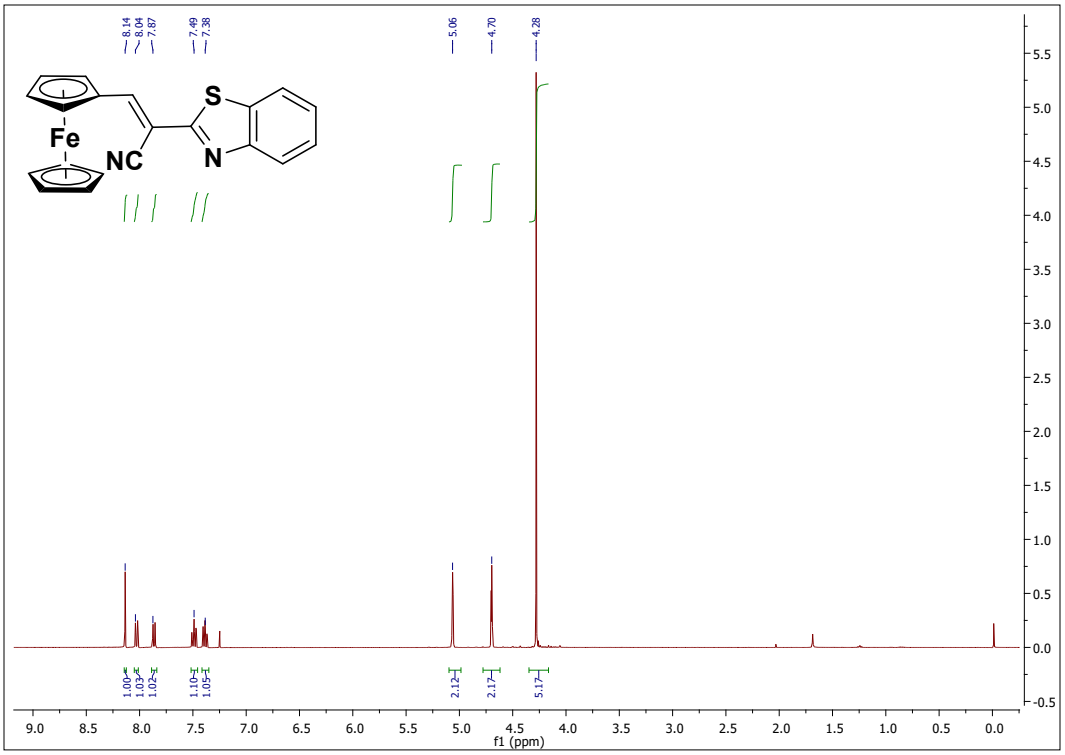

Figure S21. ^{1}H NMR spectrum (500 MHz, $CDCl_3$) of **7.**

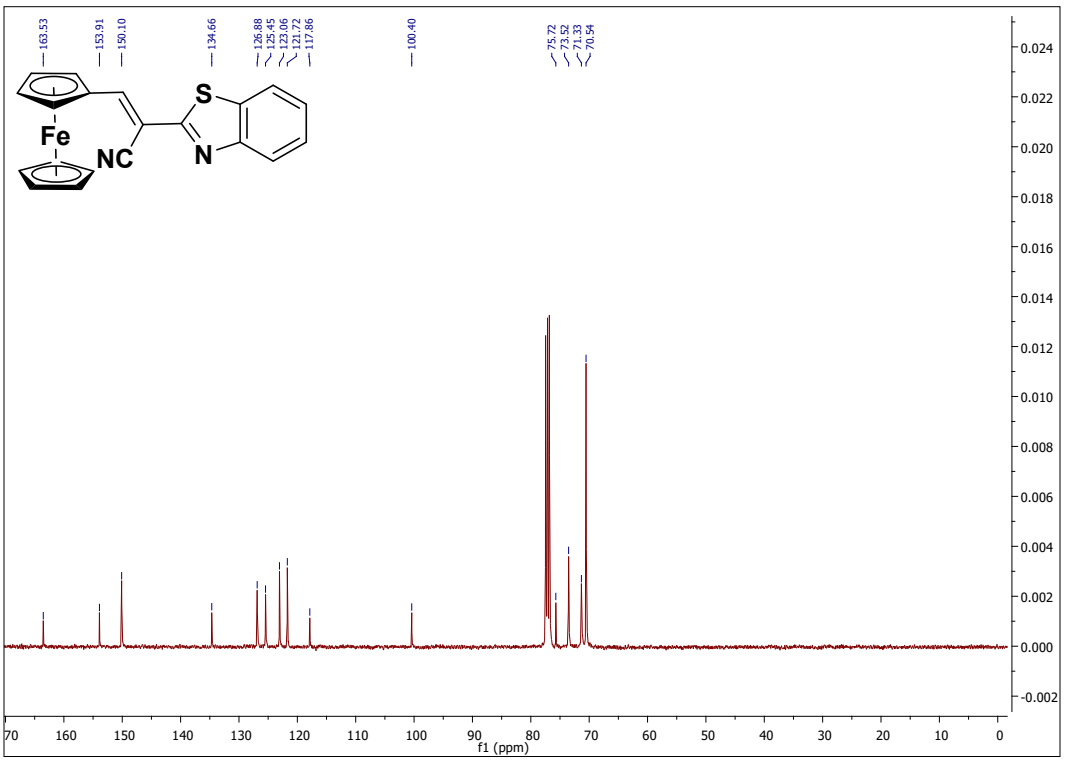

Figure S22. ^{13}C NMR spectrum (500 MHz, $CDCl_3$) of **7.**

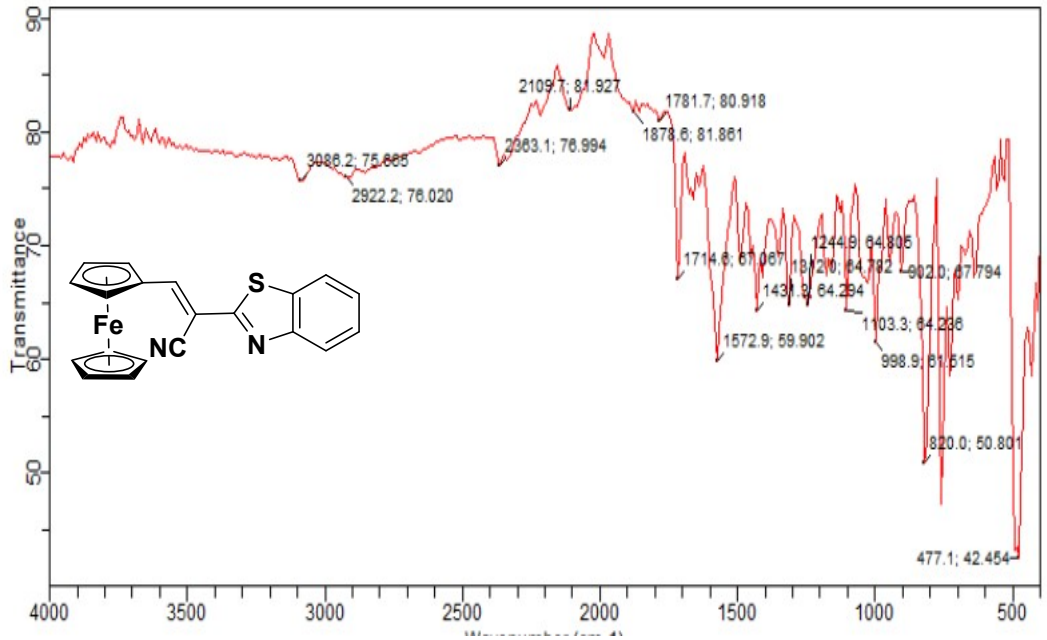

Figure S23. IR spectrum of **7.**

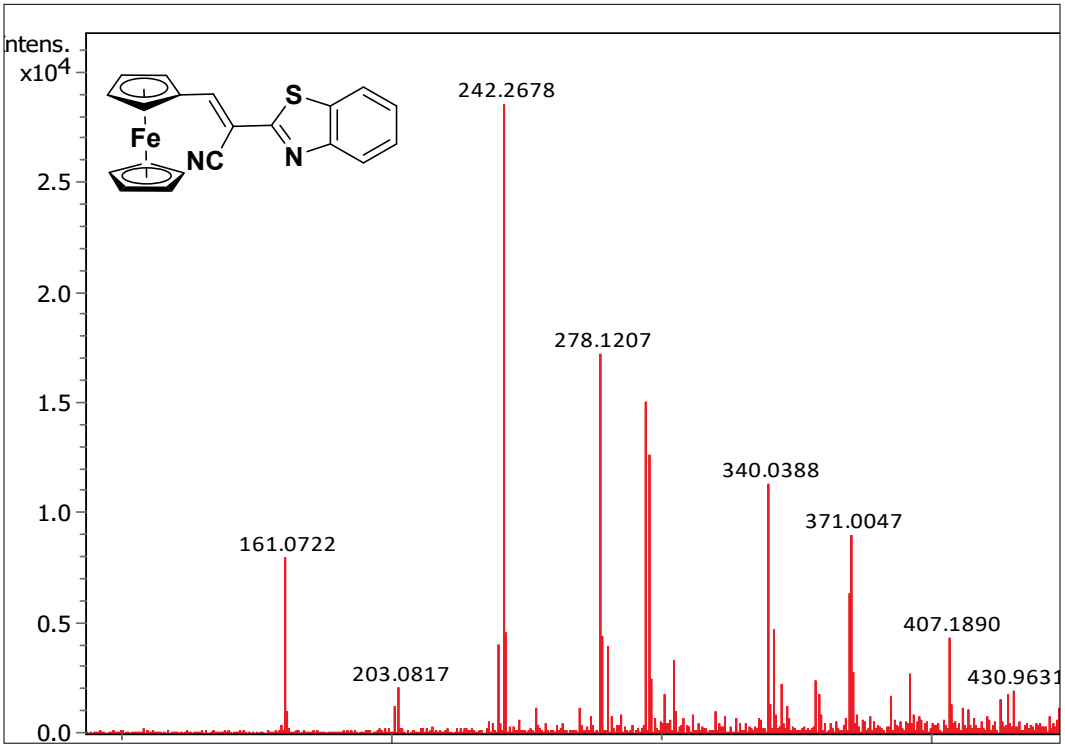

Figure S24. HRMS spectrum of **7.**

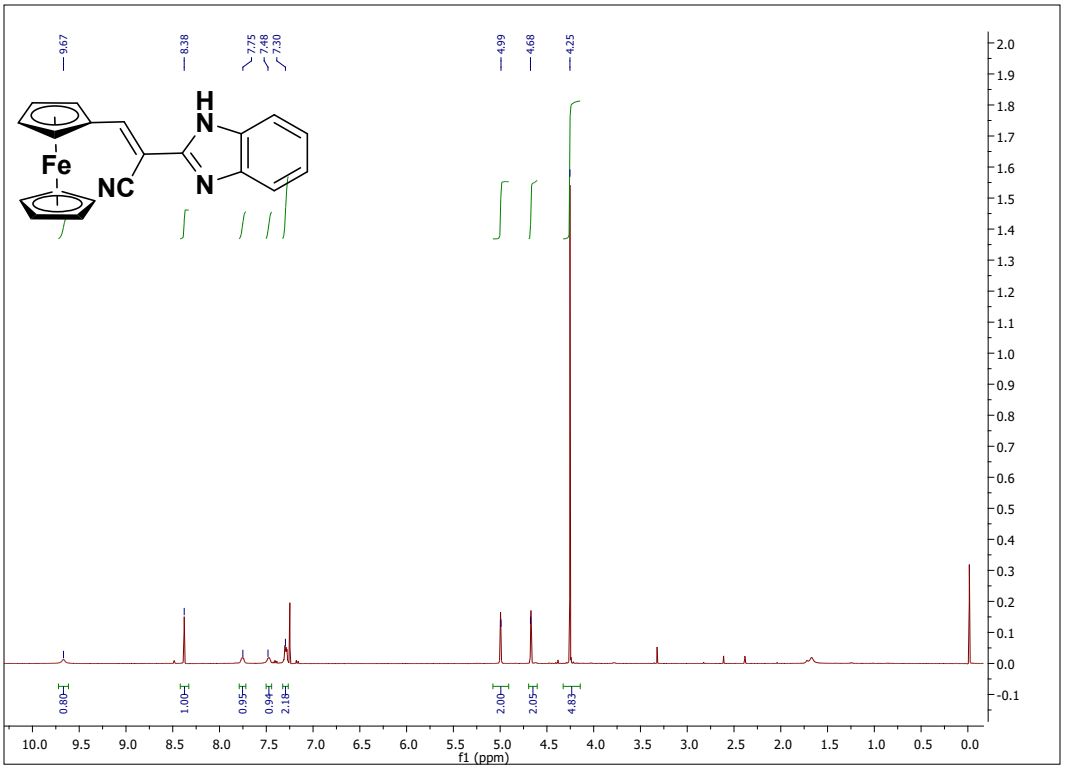

Figure S25. ^{1}H NMR spectrum (500 MHz, $CDCl_3$) of **8.**

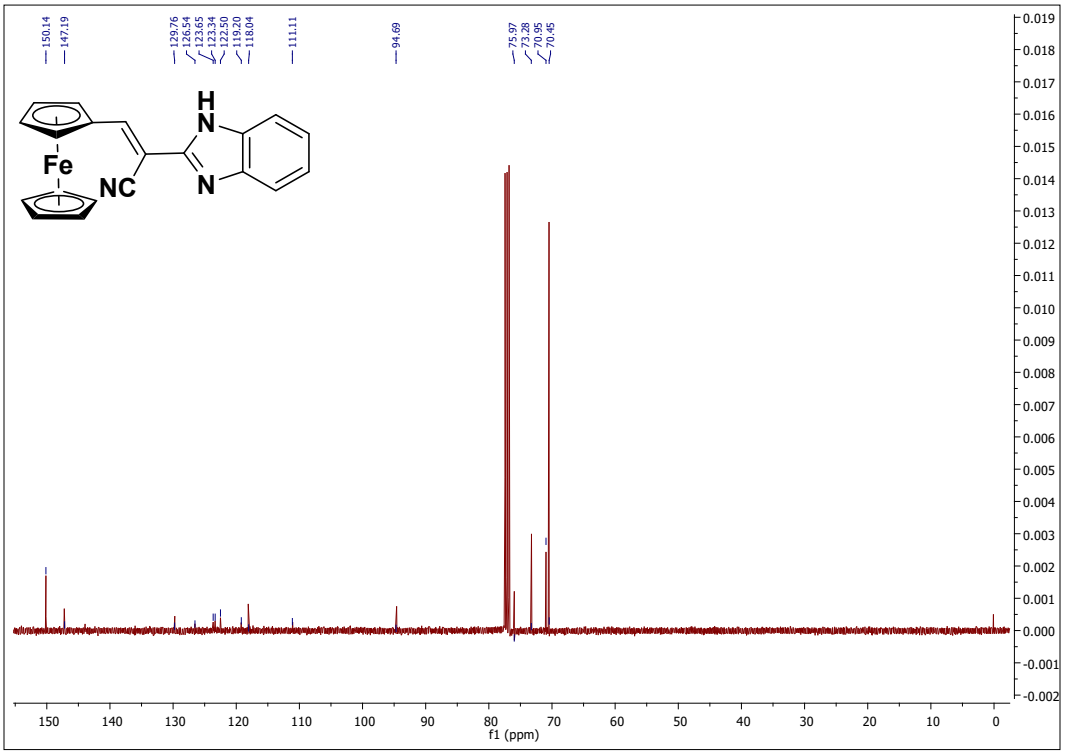

Figure S26. ^{13}C NMR spectrum (500 MHz, $CDCl_3$) of **8.**

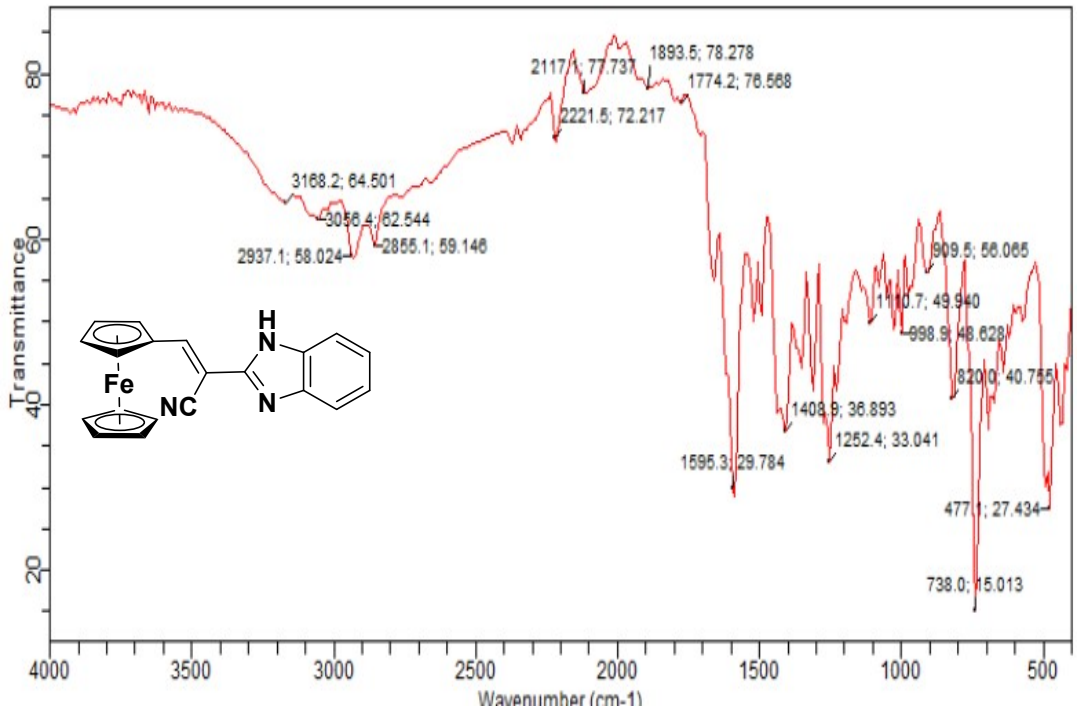

Figure S27. IR spectrum of **8.**

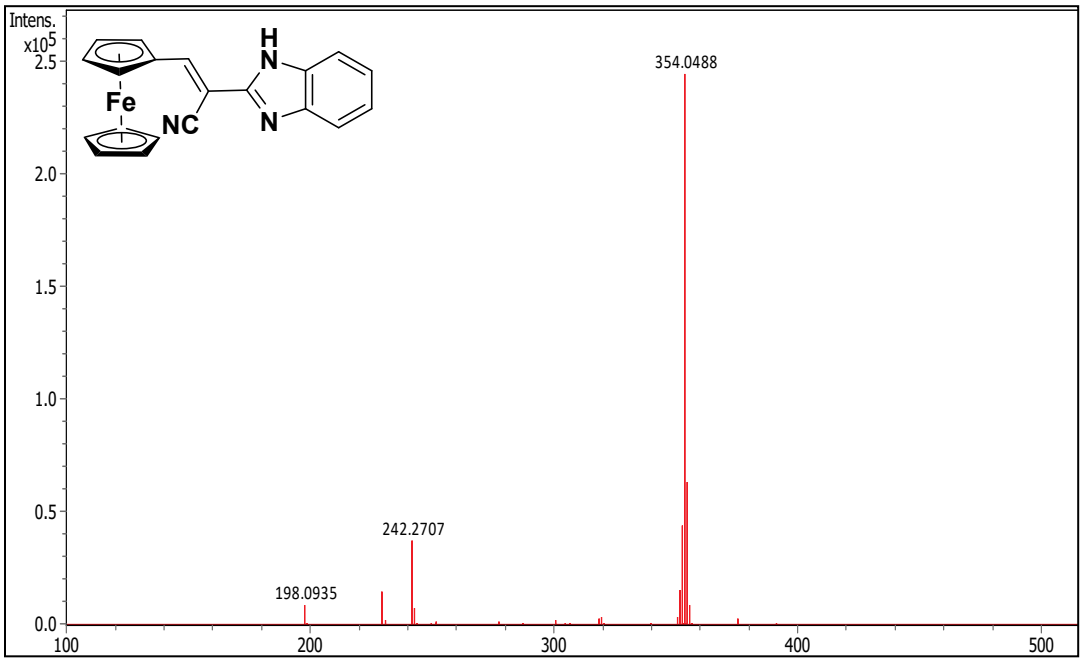

Figure S28. HRMS spectrum of **8.**

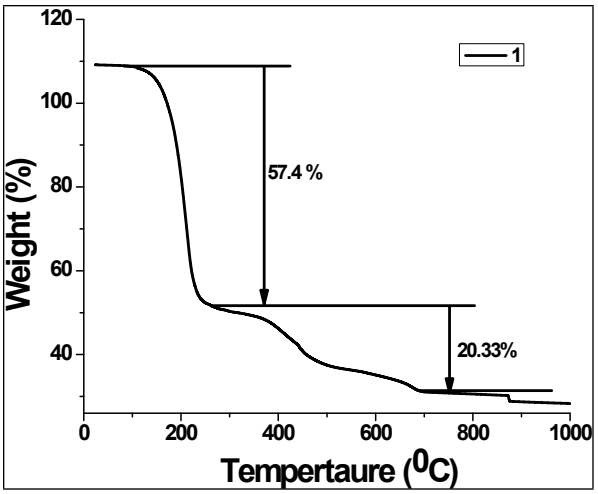
1
57.4 %
20.33%
Weight (%)
Tempertaure (^{0}C)

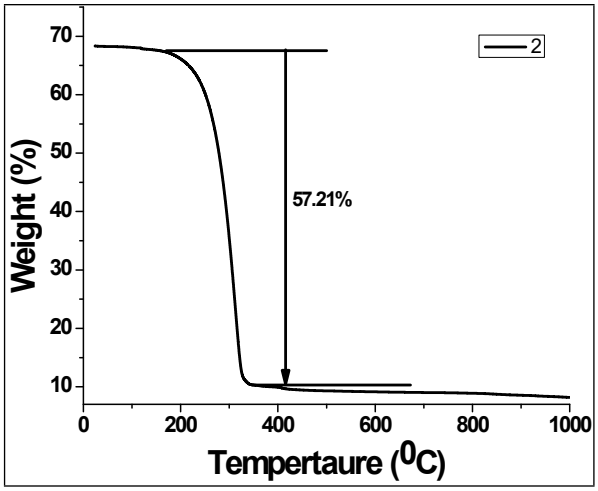
2
57.21%
Weight (%)
Tempertaure (^{0}C)

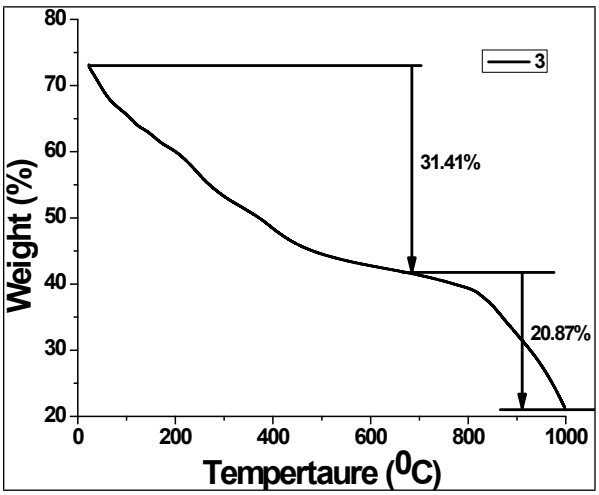
3
31.41%
20.87%
Weight (%)
Tempertaure (^{0}C)

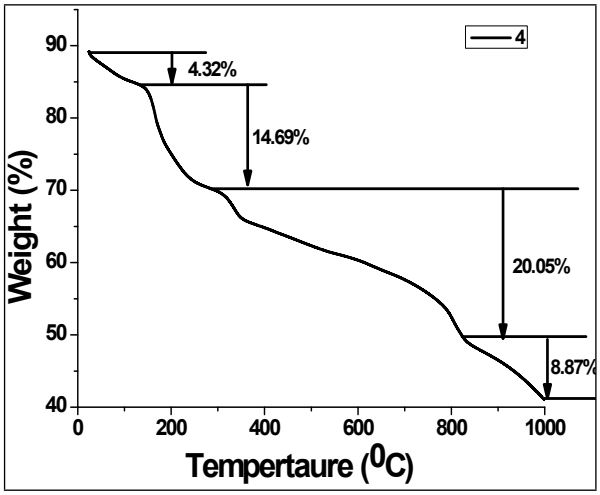
4
4.32%
14.69%
20.05%
8.87%
Weight (%)
Tempertaure (^{0}C)

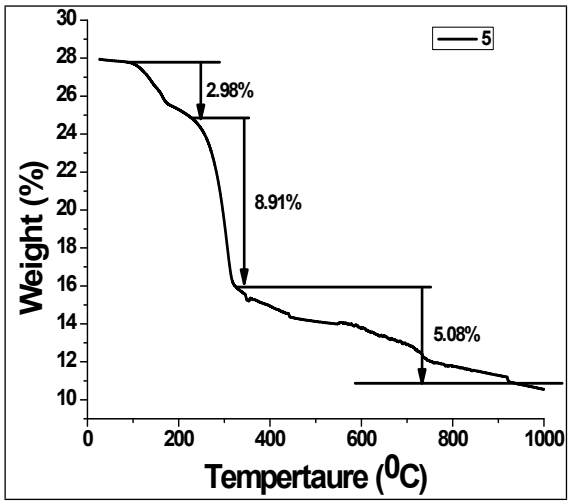
5
2.98%
8.91%
5.08%
Weight (%)
Tempertaure (^{0}C)

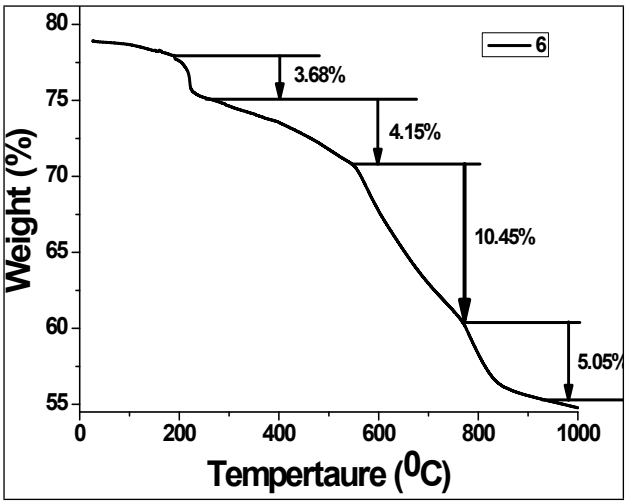
6
3.68%
4.15%
10.45%
5.05%
Weight (%)
Tempertaure (^{0}C)

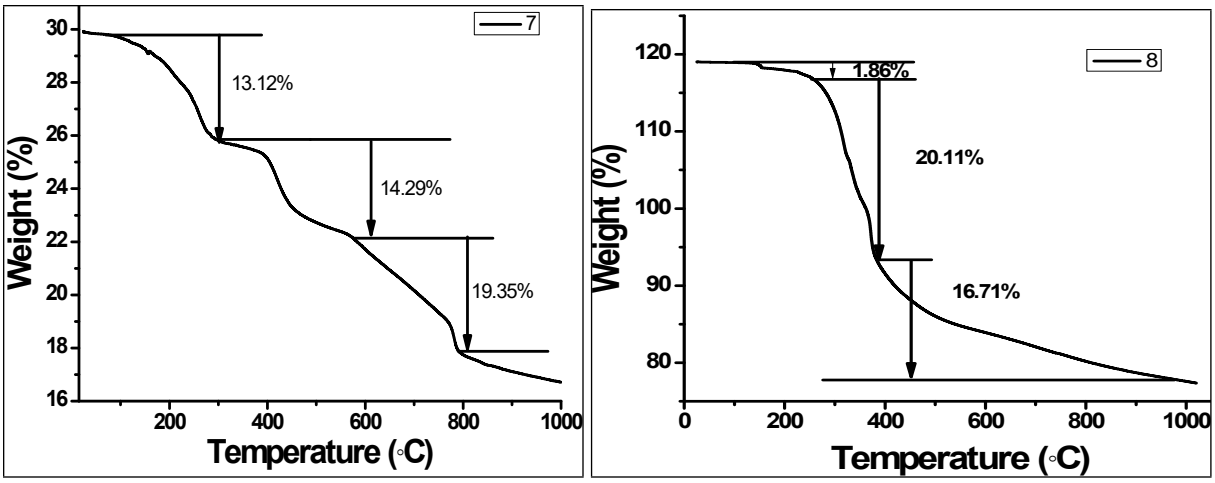

Figure S29. TGA curves of **1-8**.

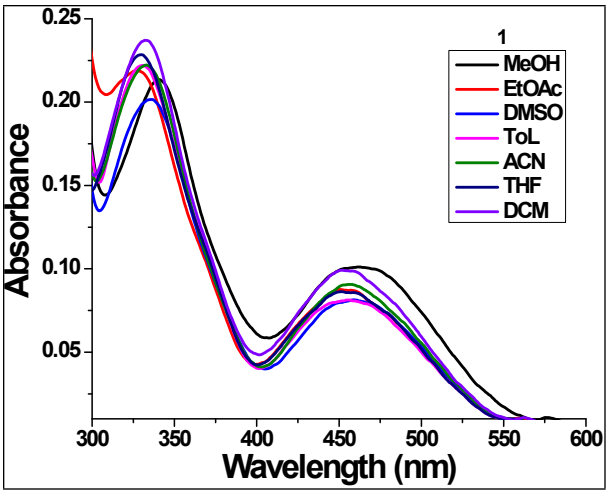
1
MeOH
EtOAc
DMSO
ToL
ACN
THF
DCM
Absorbance
Wavelength (nm)

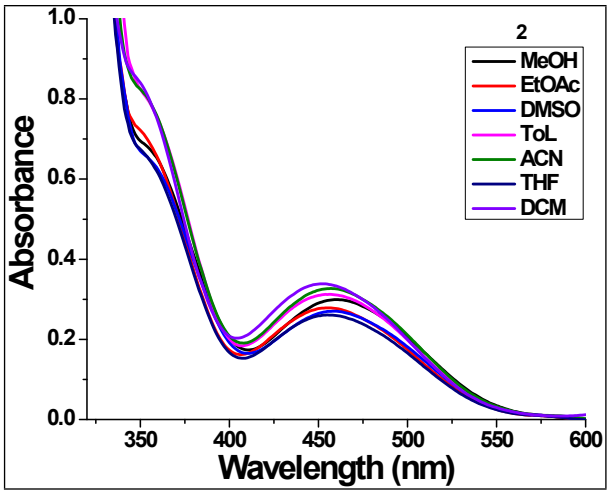
2
MeOH
EtOAc
DMSO
ToL
ACN
THF
DCM
Absorbance
Wavelength (nm)

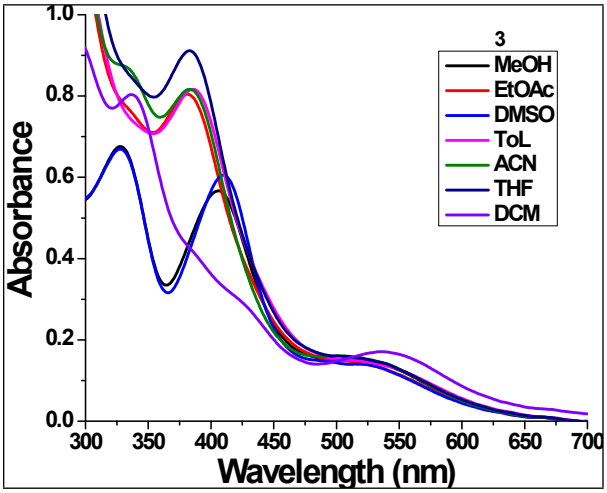
3
MeOH
EtOAc
DMSO
ToL
ACN
THF
DCM
Absorbance
Wavelength (nm)

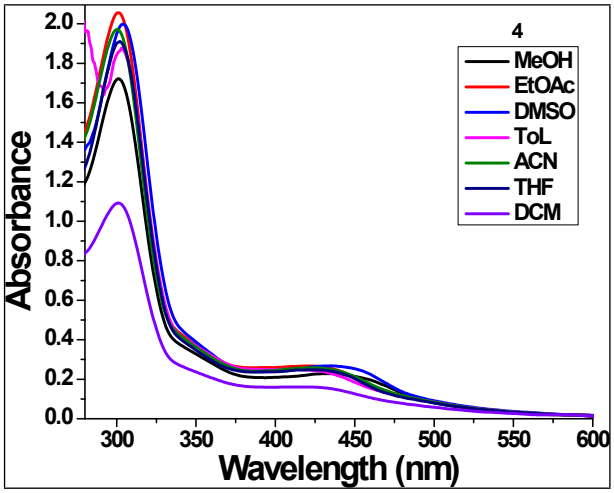
4
MeOH
EtOAc
DMSO
ToL
ACN
THF
DCM
Absorbance
Wavelength (nm)

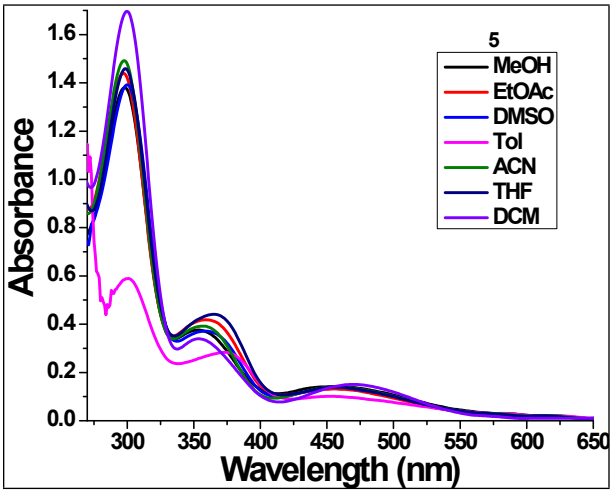
5
MeOH
EtOAc
DMSO
Tol
ACN
THF
DCM
Absorbance
Wavelength (nm)

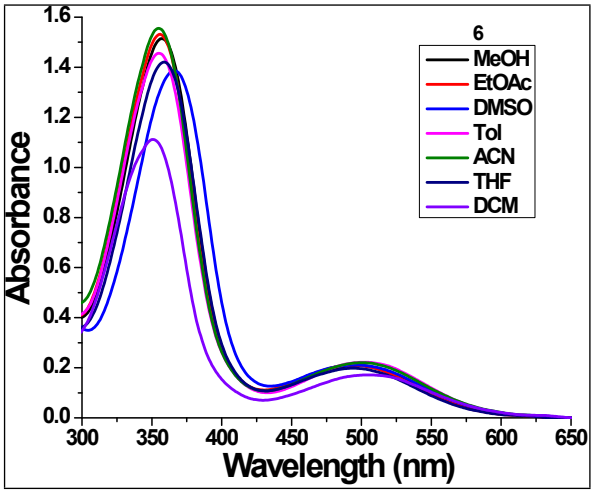
6
MeOH
EtOAc
DMSO
Tol
ACN
THF
DCM
Absorbance
Wavelength (nm)

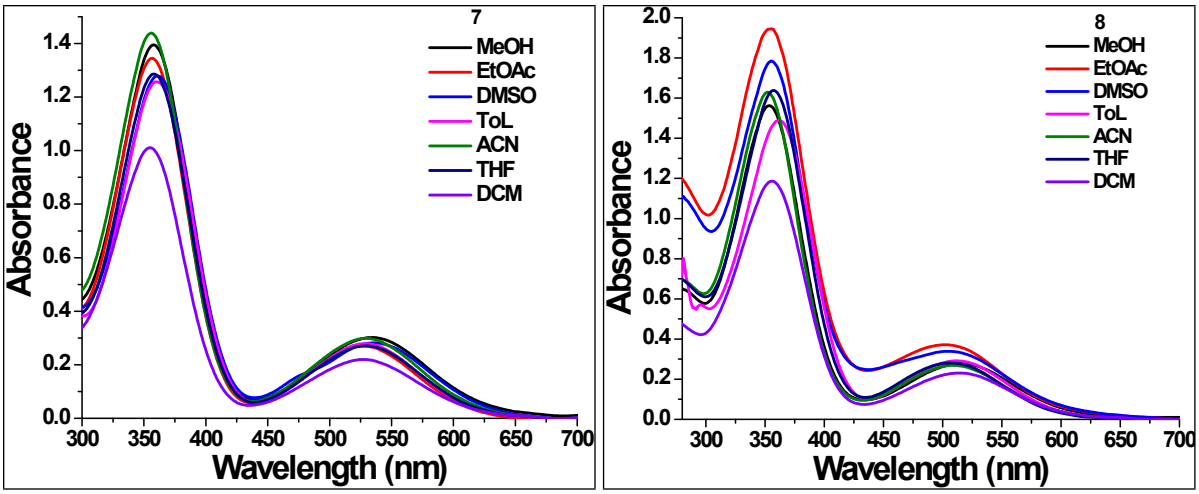

Figure S30. UV-visible absorption spectra of **1-8** in solvents of different polarity (1×10^{-4} M).

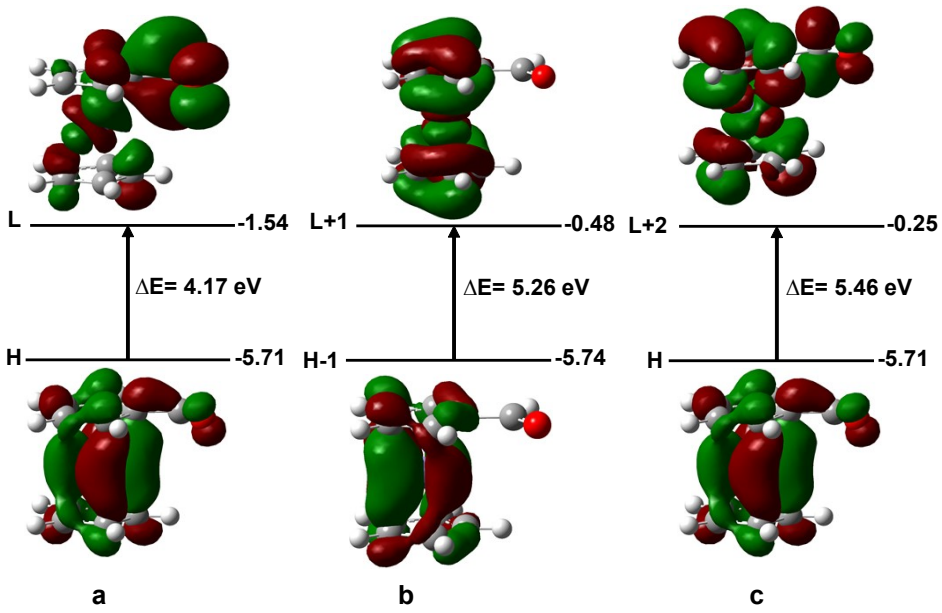

Figure S31. TD-DFT calculated electron density distributions and HOMO-LUMO energy gaps of the corresponding MLCT (a) and $\pi \rightarrow \pi^*$ (b & c) transitions of **1**.

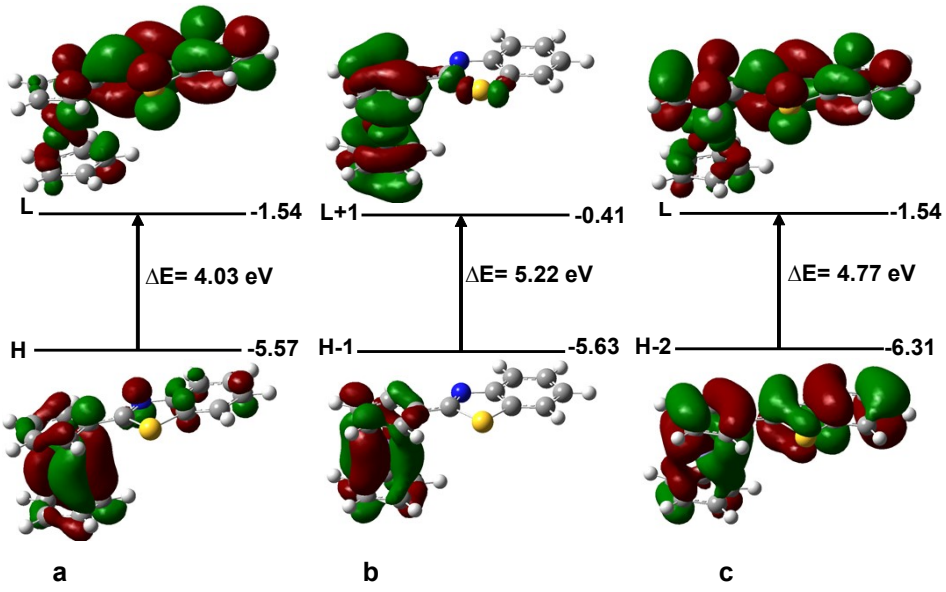

Figure S32. TD-DFT calculated electron density distributions and HOMO-LUMO energy gaps of the corresponding MLCT (a) and $\pi \rightarrow \pi^*$ (b & c) transitions of **2**.

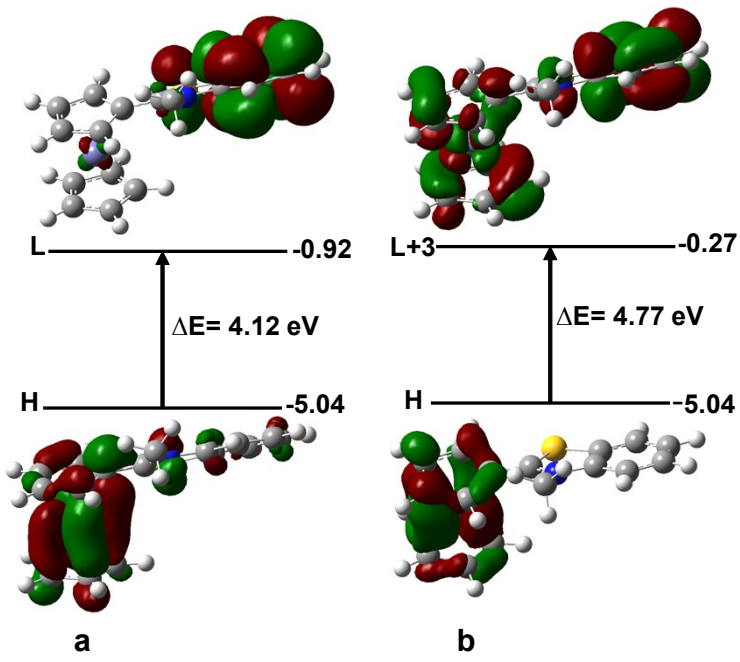

Figure S33. TD-DFT calculated electron density distributions and HOMO-LUMO energy gaps of the corresponding MLCT (a) and π→π* (b) transitions of **3**.

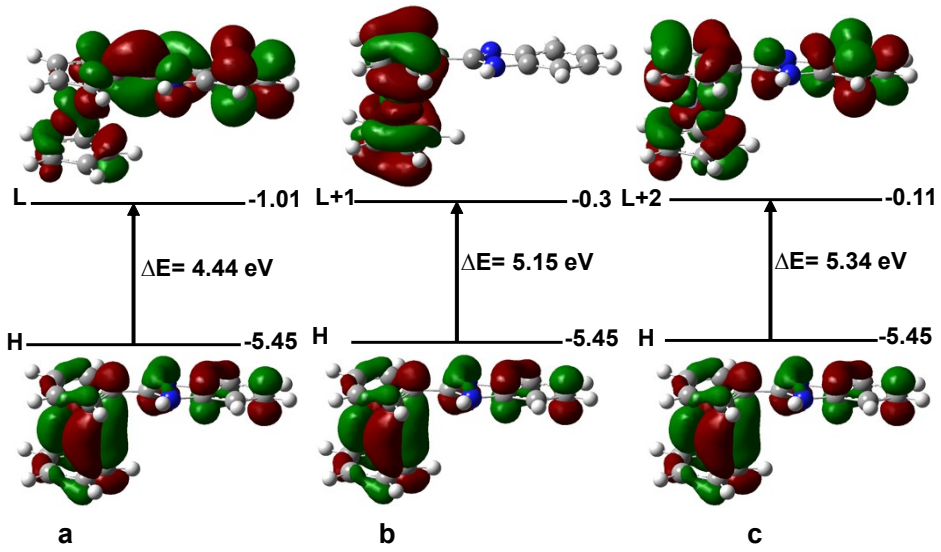

Figure S34. TD-DFT calculated electron density distributions and HOMO-LUMO energy gaps of the corresponding MLCT (a) and π→π* (b & c) transitions of **4**.

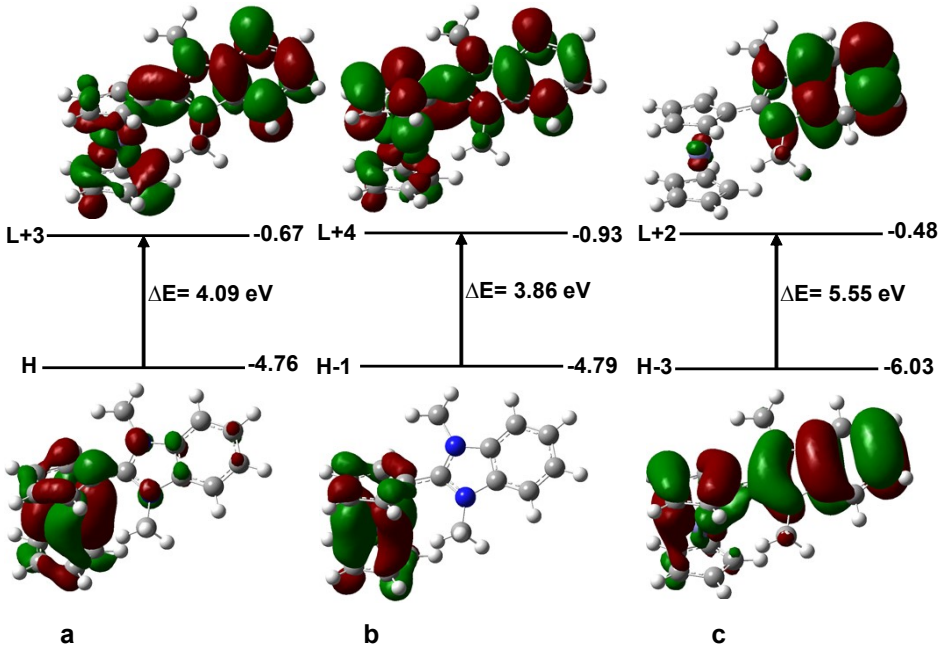

Figure S35. TD-DFT calculated electron density distributions and HOMO-LUMO energy gaps of the corresponding MLCT (a) and $\pi \rightarrow \pi^*$ (b & c) transitions of **5**.

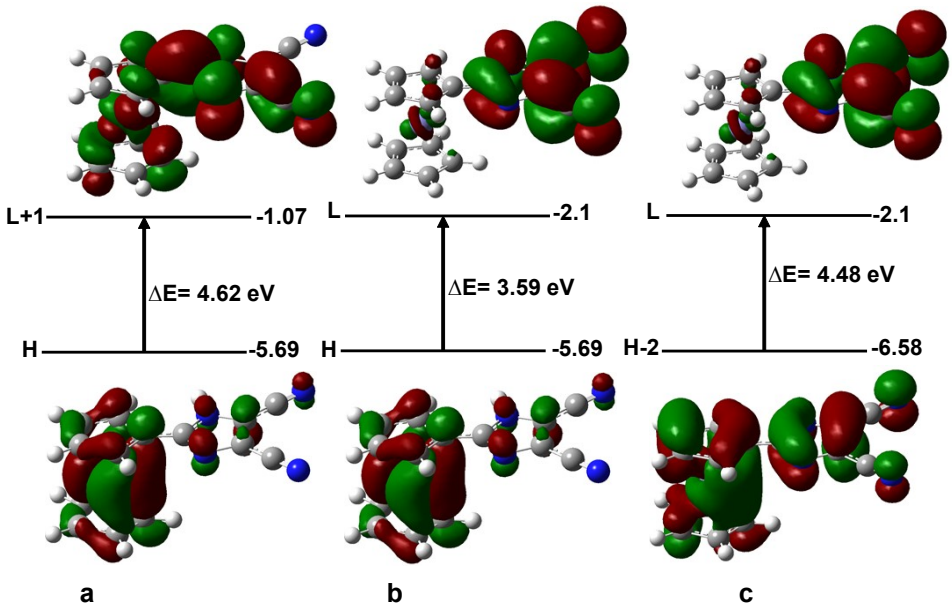

Figure S36. TD-DFT calculated electron density distributions and HOMO-LUMO energy gaps of the corresponding MLCT (a) and $\pi \rightarrow \pi^*$ (b & c) transitions of **6**.

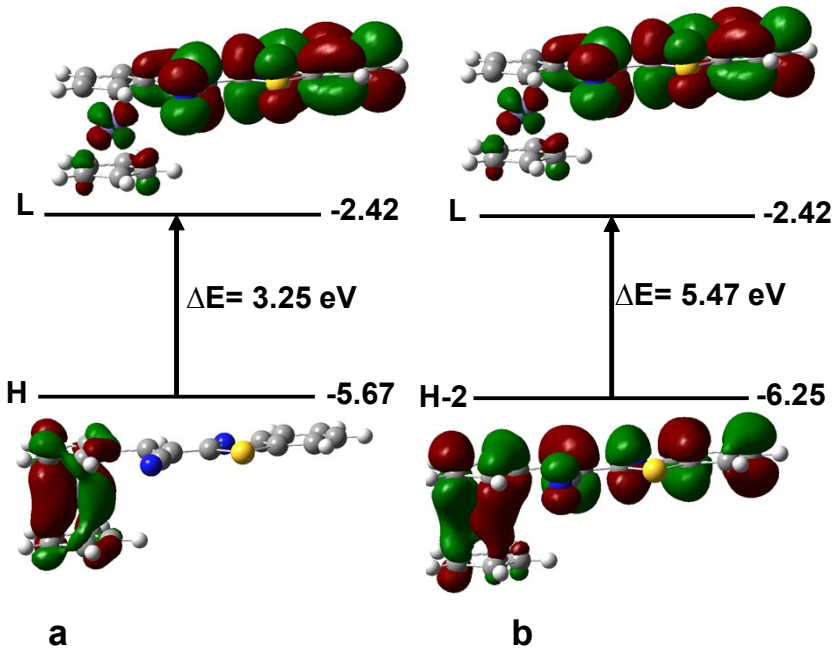

Figure S37. TD-DFT calculated electron density distributions and HOMO-LUMO energy gaps of the corresponding MLCT (a) and π→π* (b) transitions of **7**.

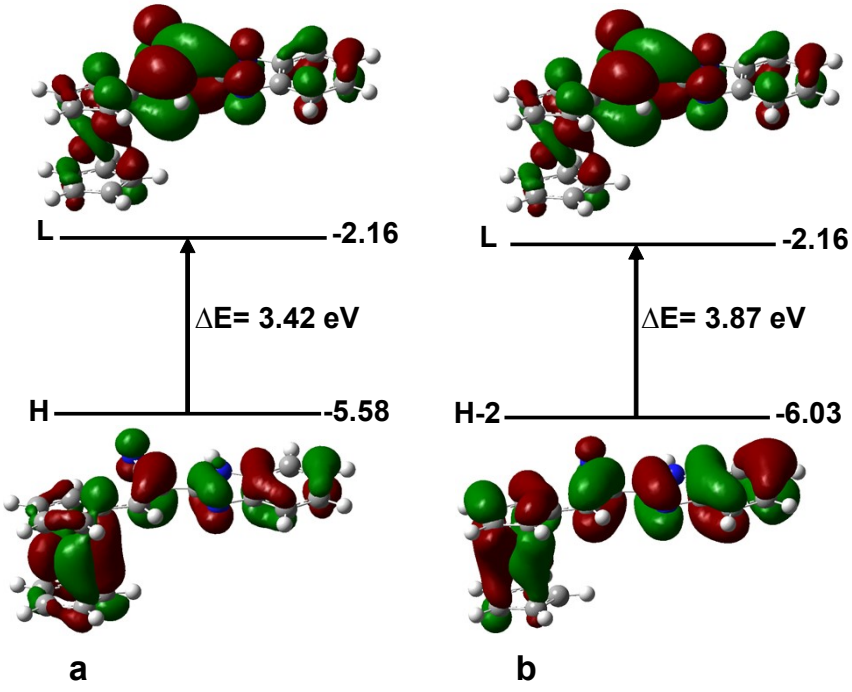

Figure S38. TD-DFT calculated electron density distributions and HOMO-LUMO energy gaps of the corresponding MLCT (a) and π→π* (b) transitions of **8**.

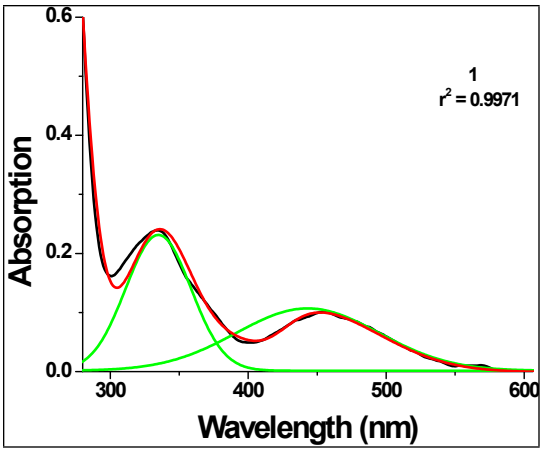
1
r² = 0.9971
Absorption
Wavelength (nm)

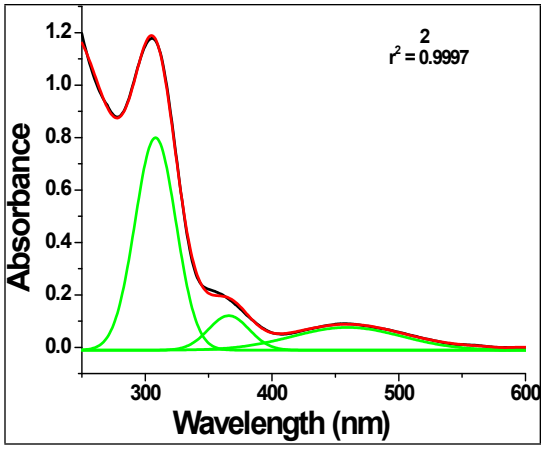
2
r² = 0.9997
Absorbance
Wavelength (nm)

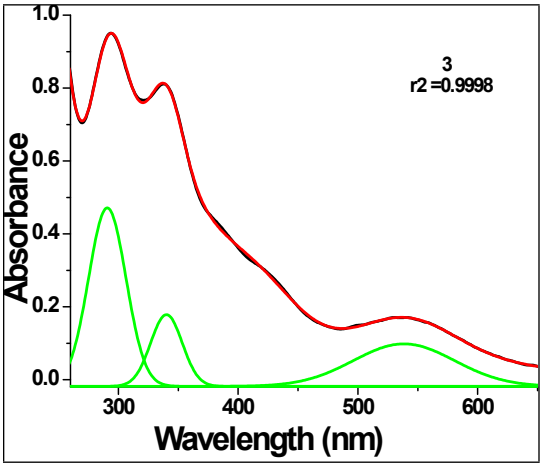
3
r2 =0.9998
Absorbance
Wavelength (nm)

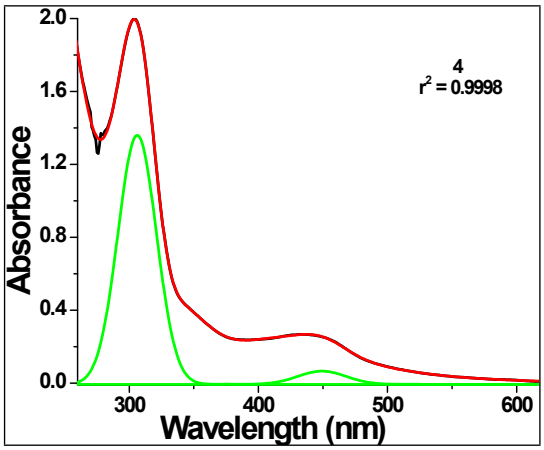
4
r² = 0.9998
Absorbance
Wavelength (nm)

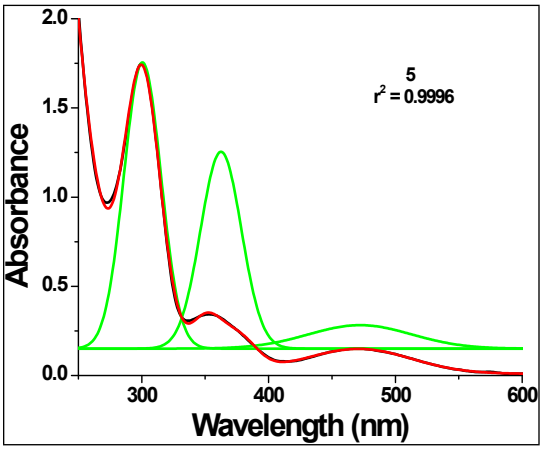
5
r² = 0.9996
Absorbance
Wavelength (nm)

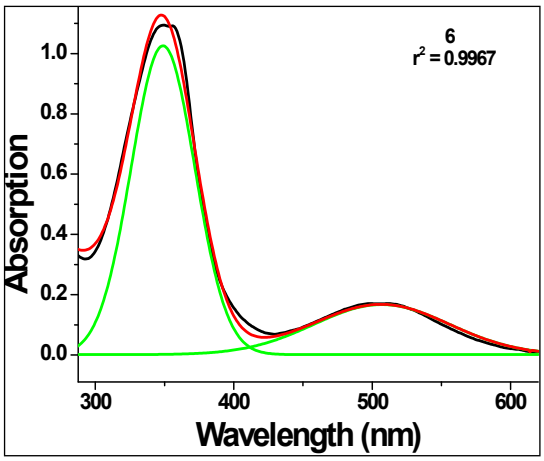
6
r² = 0.9967
Absorption
Wavelength (nm)

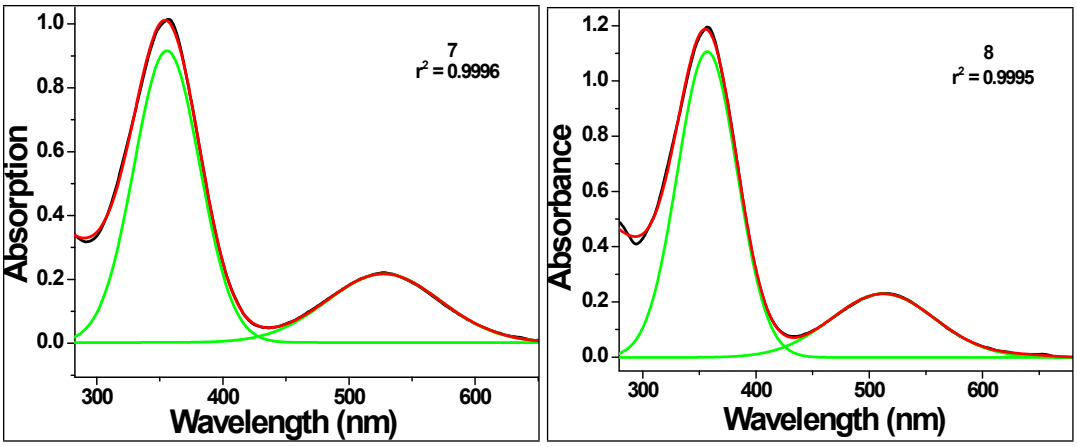

Figure S39. Band fitting curve of chromophores **1-8** in DCM at 1×10^{-4} (Red: cumulative fit peak; Black: experimental and Green: fitted peak) by using Origin Pro 8.5.

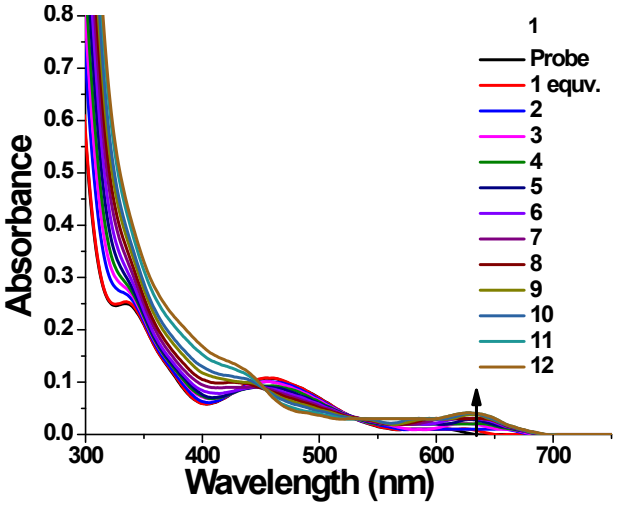
1
Probe
1 equv.
2
3
4
5
6
7
8
9
10
11
12
Absorbance
Wavelength (nm)

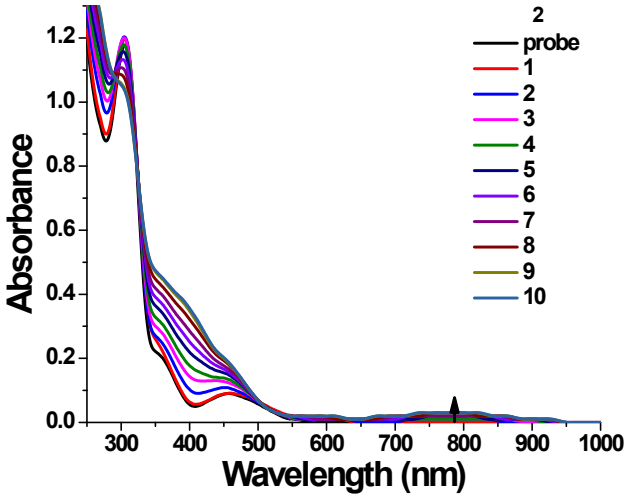
2
probe
1
2
3
4
5
6
7
8
9
10
Absorbance
Wavelength (nm)

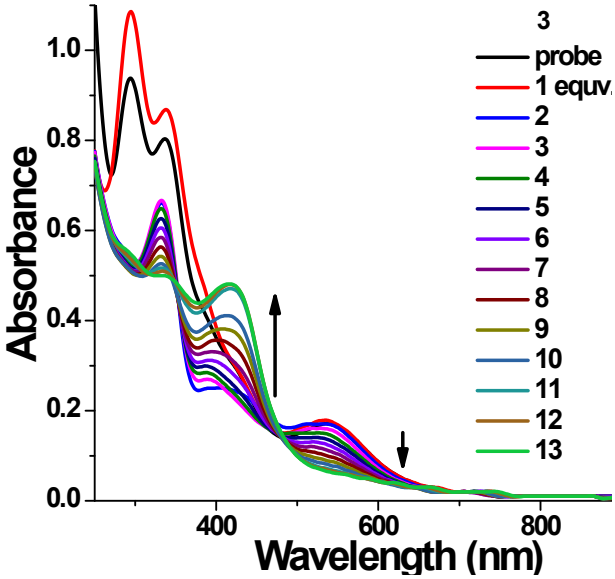
3
probe
1 equv.
2
3
4
5
6
7
8
9
10
11
12
13
Absorbance
Wavelength (nm)

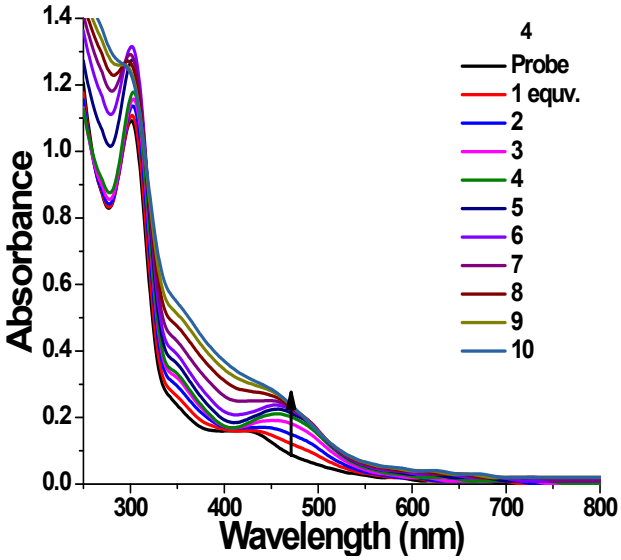
4
Probe
1 equv.
2
3
4
5
6
7
8
9
10
Absorbance
Wavelength (nm)

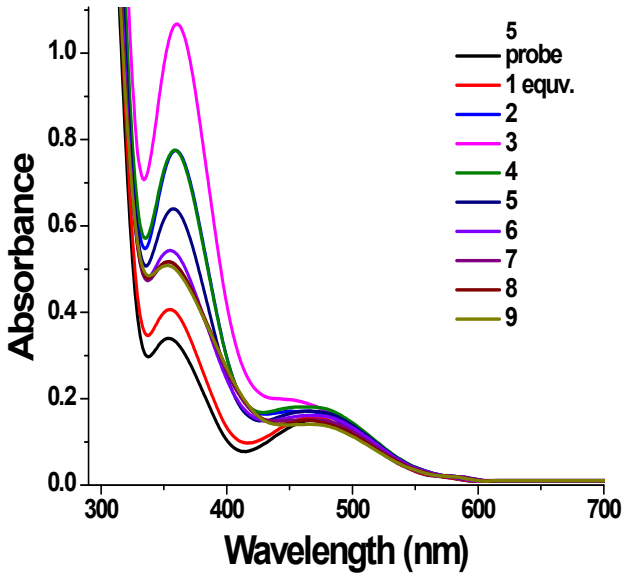
5
probe
1 equv.
2
3
4
5
6
7
8
9
Absorbance
Wavelength (nm)

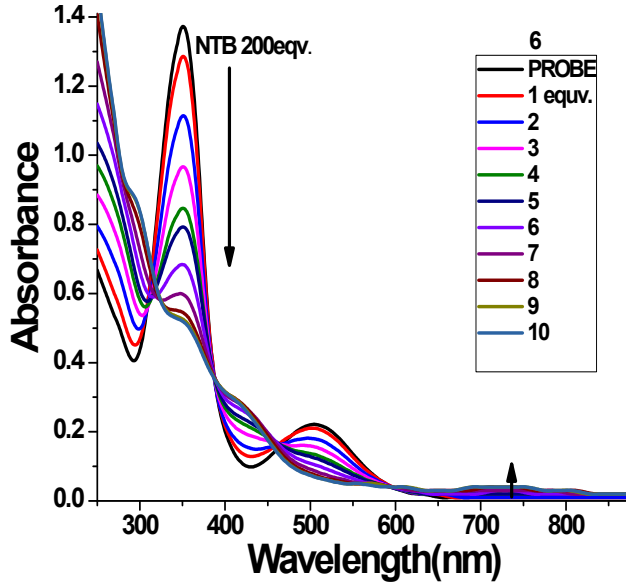
NTB 200eqv.
6
PROBE
1 equv.
2
3
4
5
6
7
8
9
10
Absorbance
Wavelength(nm)

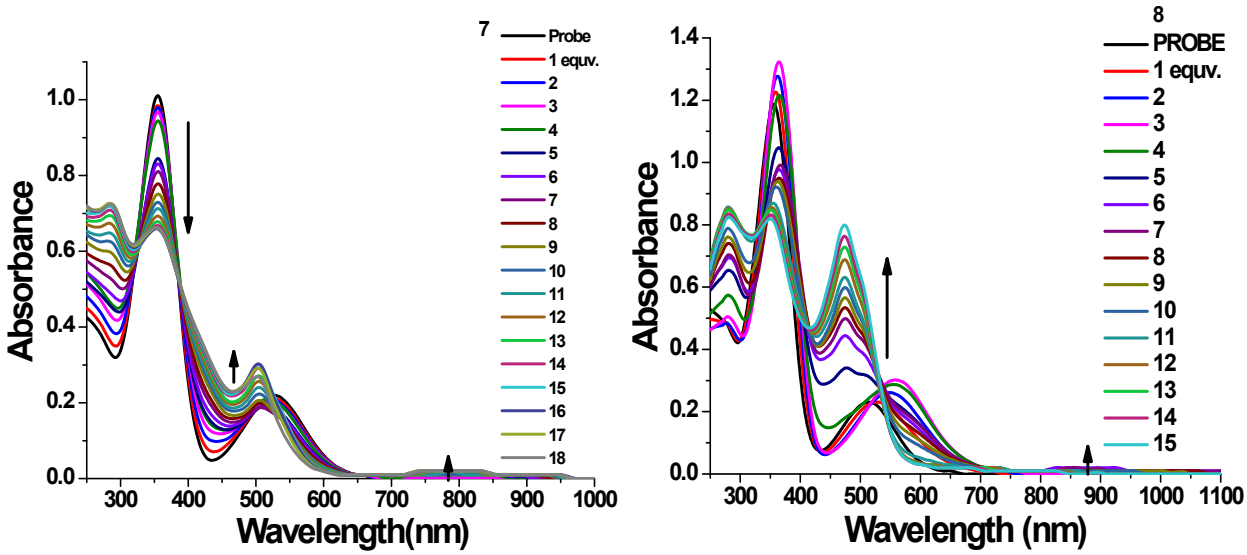

Figure S40. UV-visible absorption spectrum of **1-8** upon subsequential addition of nitronium tetrafluoroborate in dichloromethane at 1×10^{-4} M.

Complete reference no. 42

M. J. Frisch, G. W. Trucks, H. B. Schlegel, G. E. Scuseria, M. A. Robb, J. R. Cheeseman, G. Scalmani, V. Barone, G. A. Petersson, H. Nakatsuji, X. Li, M. Caricato, A. Marenich, J. Bloino, B. G. Janesko, R. Gomperts, B. Mennucci, H. P. Hratchian, J. V. Ortiz, A. F. Izmaylov, J. L. Sonnenberg, D. Williams-Young, F. Ding, F. Lipparini, F. Egidi, J. Goings, B. Peng, A. Petrone, T. Henderson, D. Ranasinghe, V. G. Zakrzewski, J. Gao, N. Rega, G. Zheng, W. Liang, M. Hada, M. Ehara, K. Toyota, R. Fukuda, J. Hasegawa, M. Ishida, T. Nakajima, Y. Honda, O. Kitao, H. Nakai, T. Vreven, K. Throssell, J. A. Montgomery, Jr., J. E. Peralta, F. Ogliaro, M. Bearpark, J. J. Heyd, E. Brothers, K. N. Kudin, V. N. Staroverov, T. Keith, R. Kobayashi, J. Normand, K. Raghavachari, A. Rendell, J. C. Burant, S. S. Iyengar, J. Tomasi, M. Cossi, J. M. Millam, M. Klene, C. Adamo, R. Cammi, J. W. Ochterski, R. L. Martin, K. Morokuma, O. Farkas, J. B. Foresman, and D. J. Fox, Gaussian, Inc., Wallingford CT, **2016**.

References:

1. D. Verreault, K. Moreno, E. Merlet, F. Adamietz, B. Kauffmann, Y. Ferrand, C. Olivier, and V. Rodriguez, *J. Am. Chem. Soc.,* **2019,** *142(1)*, 257-263.